

Effect of an intense electromagnetic field on a weakly bound system

Howard R. Reiss

*Department of Physics, University of Arizona, Tucson, Arizona 85721**
and Department of Physics, The American University, Washington, D. C. 20016†

(Received 27 April 1979; revised manuscript received 16 July 1980)

The approximation method introduced by Keldysh is revised and extended. The technique is applicable to the photodetachment by a plane-wave field of an electron bound by a short-range potential. The approximation is to neglect the effect of the binding potential as compared to the field effects on the final state of the detached electron. By choice of a different gauge than that used by Keldysh, the formalism becomes very simple and tractable. A general basis for the formalism is developed, and it is then applied to find transition probabilities for any order of interaction for both linearly and circularly polarized plane-wave fields. The low-intensity, first-order limit and the high-intensity, high-order limit yield the correct results. Two intensity parameters are identified. The fundamental one is $z = e^2 a^2 / 4m\omega$, where a is the magnitude of the vector potential (in radiation gauge) of the field of circular frequency ω . The second parameter is $z_1 = 2z\omega / E_B$, where E_B is binding energy, and it becomes important only in the asymptotic case. With the assumption that the field leaves the neutral atomic core relatively unaffected, the formalism is applied to the example of the negative hydrogen ion irradiated by circularly or linearly polarized 10.6- μm radiation. Photodetachment angular distributions and total transition probabilities are examined for explicit intensity effects. It is found that total transition probability W is not sensitive to intensity since $d(\log W)/d(\log z)$ retains low-intensity straight-line behavior up to quite high values of z . An important intensity effect is the major significance of higher-than-lowest-order terms when z is large, especially for circular polarization. A sensitive indicator of intensity is the ratio of photodetachment probabilities in circularly and linearly polarized fields, which increases sharply with intensity. An investigation of the convergence of perturbation expansions gives the upper limit $z < [E_B / \omega] - E_B / \omega$, where the square bracket means "smallest integer containing" the quantity in brackets. This limit is $z < 0.59$ for H^- in 10.6- μm radiation. The failure of perturbation theory is not necessarily manifest in qualitative ways. For example, it is not apparent in total photoelectron yield as a function of intensity.

I. INTRODUCTION

The physical problem treated here is the action of an external plane-wave electromagnetic field on an electron bound by a finite-range potential. The applied field may be very intense, although there are practical limits to the intensity which can be considered. The approach is entirely analytical. The technique is based on a combination of solutions for the electron in the applied field alone, without the binding potential, and on solutions for the electron in the binding potential alone, without the applied field. An important aspect of the work is the availability of closed-form analytical solutions within the context of assumptions on the finite range of the binding potential and the absence of intermediate-state resonances.

The work reported here is closely related to that of Keldysh.¹ An essential difference between the present work and the Keldysh work is in the choice of gauge in which the external electromagnetic field is expressed. Keldysh used electric field gauge, where the interaction Hamiltonian is $-e\vec{F} \cdot \vec{r}$ (where \vec{F} is the electric field vector); whereas radiation gauge is used below, with an interaction Hamiltonian $-m^{-1}e\vec{A} \cdot (-i\vec{\nabla}) + (2m)^{-1}e^2\vec{A}^2$ (where \vec{A} is the vector potential of the applied field). Throughout this paper, the convention $\hbar = c = 1$ is

used. The analytical advantages attached to the use of radiation gauge are major. For instance, Keldysh is forced to resort to a low field-frequency (or large photon-order) approximation early in his work, so that the low-order perturbation theory limit is not accessible from his results.²⁻⁴ The simplicity attendant upon the use of radiation gauge permits the development of a general analytical expression which contains the proper high- and low-order limits, and also makes available other general results with far-reaching implications. Radiation gauge was used by Jones and Reiss⁵ to calculate multiphoton interband transitions in solids induced by circularly polarized radiation. The correct perturbation limit is obtained by them. A general discussion of the advantages of radiation gauge for intense-field problems is given in Ref. 6.

In Sec. II, the Keldysh approximation for the S matrix is presented. This approximation replaces the complete interacting state for the photodetached particle by a state in which field effects are retained in full, but binding effects are neglected. A qualitative discussion is given to show that this approximation can be viewed as arising from an expansion in the binding potential, and should be much superior to a conventional perturbation expansion in the external field when field intensity is high and the range of the binding poten-

tial is short.

The S matrix derived in Sec. II is used in Sec. III for the calculation of a general differential transition probability per unit time, and total transition probability per unit time for photodetachment of an electron bound by a finite-range potential. Both circular and linear polarization of the applied field are considered. The expressions are found to depend on a general intensity parameter $z = e^2 a^2 / 4m\omega$, where a is the amplitude of the radiation-gauge vector potential of the applied plane-wave field of circular frequency ω . The results are in closed analytical form, and, within the approximations inherent in the S matrix employed, are valid for all multiphoton orders and all intensities. In practical application, intensities will be limited to values sufficiently low that significant depletion will not occur in the irradiated sample. Also, it is generally presumed that the intensity is not so high that photodetachment occurs before asymptotic-time behavior of the expression for transition probability per unit time can develop. This last restriction is not particularly limiting, as is discussed in detail in a later section.

The low-intensity limit of the transition probability per unit time is found in Sec. IV. For transitions which are first order in the applied field, the results are identical to those derivable directly from first-order perturbation theory. The low intensity limit for arbitrary multiphoton order is obtained readily for the case of circular polarization of the applied field. The linear polarization case is also developed, but it presents extra complications because of the presence in that case of a generalized Bessel function of two variables. The properties of this function are given in the Appendices. A general comparison of transition probabilities for circular as compared to linear polarization as a function of E_B/ω is also given in Sec. IV, where E_B is the binding energy of the electron.

Asymptotic results for large values of the intensity parameter, z , are given in Sec. V. The energy conservation condition contains the intensity parameter in such fashion that the condition $z \gg 1$ requires also that the minimum multiphoton order be large. The asymptotic forms thus obtained are relatively complicated, but if a second intensity parameter, z_1 , is large, then the simple tunneling form occurs. This second intensity parameter is $z_1 = 2z\omega/E_B$, where E_B is the binding energy of the electron. The z_1 parameter is just the inverse square of the Keldysh¹ intensity parameter γ . Because Keldysh used a large multiphoton-order approximation from the outset, his work does not contain the more fundamental intensity

parameter, z .

The important problem of the time required for the transition probability expression to reach its infinite-time analytical form is explored in Sec. VI. To reduce algebraic complication, attention is confined to the simpler circular polarization case. It is found that the condition for asymptotic-time behavior is essentially $\omega t \gg 1$. That is, the condition is essentially that the time be much in excess of a single wave period. With the further limitation that transition probabilities should be constrained to sufficiently small values that depletion effects do not occur within a single pulse of the applied radiation, the asymptotic-time behavior is guaranteed. The results about asymptotic times contradict results obtained by Geltman.⁷ However, Geltman's technique was to consider an intense oscillatory electric field in a one-dimensional framework, which is fundamentally different from the intense-field plane-wave case. The magnetic field component of a plane wave is important at high intensity, but Geltman's work has no magnetic field. The physical problems are different.

An application of the formalism developed in this paper to a concrete example is given in Sec. VII. The example chosen is the photodetachment of the excess electron from an H^- ion by 10.6- μ m plane-wave radiation, either circularly or linearly polarized. Effects of the field on the neutral atomic core of H^- are neglected. The bound-state wave function of H^- is represented by a simple analytical approximation given by Armstrong.⁸ The differential transition probability per unit time is given in closed analytical form. Integration over the solid angle to get the total transition probability per unit time is done numerically. The angular distributions of photodetached electrons are strikingly different in circular and linear polarization cases. Circular polarization results always peak in the sideways direction (with respect to an axis along the direction of propagation of the field). Linear polarization results exhibit several peaks, with the largest peak in the forward direction for odd multiphoton orders, but not for even multiphoton orders (where the axis is oriented along the polarization direction). The effect of intensity on the shape of the angular distribution is modest for circular polarization, but striking for linear polarization. On the other hand, the curves found for total transition probability per unit time as a function of intensity do not show major deviations for either polarization from the trend which would be expected from low-intensity perturbation theory.⁹ That is, the total transition probability per unit time (or total cross section) is not a sensitive indicator

of intensity effects. If angular distributions are measured, the linear polarization case is sensitive to intensity. Another way to detect explicit intensity effects is accessible if the energy of the detached electrons is measured. When intensity is low, of course, only the minimum multiphoton order contributes, and the electron spectrum is monochromatic. However, as intensity increases, there are major contributions from higher-than-lowest multiphoton orders, and significant extra energy can be imparted to some of the detached electrons. This effect is strongly dependent on intensity, and is more striking with circular than with linear polarization of the field. There is another explicit intensity effect which does not require measurement either of angular distributions or of electron energies. If one takes the ratio of the total yield of photoelectrons as detached by circularly as compared to linearly polarized radiation, that ratio is independent of intensity until about $z = 10^{-2}$ is reached. The ratio then rises sharply with intensity. Specifically the ratio of circular to linear polarization yields is quite small at low intensity, as would be expected¹⁰ with a relatively large multiphoton order. However, the low-intensity ratio of 10^{-3} is increased by a factor of 10^2 as the intensity increases to about $z = 2.4$. This intensity effect has not been remarked upon previously.

Section VIII gives a very brief treatment of the application of the formalism to the neutral H atom. Although this is the example selected by Keldysh,¹ the formalism is of very limited validity for this problem.

Section IX is devoted to an investigation of the convergence of perturbation theory in the presence of circularly polarized radiation. The analytical expression for differential transition probability per unit time lends itself to a very straightforward examination for singularity structure in the complex intensity parameter plane. The intensity parameter, z , is the expansion parameter of perturbation theory. The radius of convergence of perturbation theory is found to be limited by an essential singularity at $z = [E_B/\omega] - E_B/\omega$, where the square bracket signifies the smallest integer containing the quantity in the bracket. For the example of H^- irradiated by a $10.6\text{-}\mu\text{m}$ field, this limit on perturbation theory is $z < 0.59$. A plausibility argument is given to show that the correction terms which were omitted from the S matrix which was used are of such a nature that they cannot cancel the essential singularity which limits perturbation theory. If this inference is correct, the limit found on the radius of convergence of perturbation theory is an upper bound for this H^- problem, which can only be de-

creased by binding-potential corrections to the theory given here. Although the limits given here are for the H^- problem, they are easily found for any finite-range potential by insertion of the appropriate momentum-space wave function in the transition probability expression. In principle, limits on perturbation expansions can be found also for linearly polarized fields, but the presence of the generalized Bessel functions of two variables makes the analysis very much more difficult.¹¹

II. S-MATRIX FORMALISM

The general physical problem considered here is one in which a charged particle (nominally considered to be an electron), initially bound to a center of force by a finite-range potential, experiences detachment from the center of force through the action of an intense plane-wave electromagnetic field. The S matrix to describe the photodetachment can be written in general as

$$S_{fi} = \lim_{t \rightarrow -\infty} (\Psi_f^{(-)}, \Phi_i), \quad (1)$$

where $\Psi_f^{(-)}$ is the final out-state of the system containing the complete effects of the electromagnetic field as well as the binding potential, while Φ_i is the initial state of the unperturbed system with no field present. [The form given is more convenient than the alternative form $S_{fi} = \lim_{t \rightarrow -\infty} (\Phi_f, \Psi_i^{(+)})$, because Φ_i in Eq. (1) is the initial, unperturbed, bound state, which is unique and well-known; whereas Φ_f would be one of a set of unbound states. Furthermore, $\Psi_f^{(-)}$ in Eq. (1) can reasonably be assumed to be dominated by the applied field, whereas no such assumption can be made for $\Psi_i^{(+)}$.] By using the integral-equation solution for $\Psi_f^{(-)}$, one can write Eq. (1) as

$$S_{fi} = \delta_{fi} - i \int_{-\infty}^{\infty} dt_1 (\Psi_f^{(-)}, V_A \Phi_i)_{t_1}, \quad (2)$$

where V_A represents the interaction potential due to the applied electromagnetic field, and the subscript t_1 on the scalar product means that all factors in the product depend on t_1 . The steps necessary to pass from Eq. (1) to Eq. (2) are described in Appendix A. The approximate form of the S matrix to be used in this paper follows from the assumption that, after detachment by the intense electromagnetic field, the state of the initially bound particle is adequately described by the state vector in which only the effects of the applied field are considered, and the binding potential is ignored. That is, Eq. (2) is rewritten as

$$(S - 1)_{fi} \approx -i \int dt_1 (\Psi_A, V_A \Phi_i)_{t_1}, \quad (3)$$

where Ψ_A is the state vector for the free charged particle in the presence of the electromagnetic

field—i. e., the Volkov state vector. Equation (3) is the basic approximation employed in this paper. This is exactly the Keldysh approximation.¹

Other approximations could also be used as a starting point in place of Eq. (3). For instance, one could substitute for $\Psi_f^{(-)}$ in Eq. (2), a state vector corresponding to a continuum state of a particle in the presence of the binding potential, but with no effects of the applied field considered. This would be more in line with conventional perturbation theory. Equation (3) is superior to this other possibility, and some further insight into the reasons for that can be obtained from results in Appendix A. A formal development is given in Appendix A for the case where a particle bound by potential V_B is affected by the introduction of the potential V_A , representing the applied field. The formalism so developed is not strictly applicable to the physical problems to be considered in this paper, since V_B will be modified by the external field, whereas the assumption that V_A and V_B are independent is inherent in Appendix A. To give a specific example, suppose the physical process being explored is the photodetachment of a negative hydrogen ion. Certainly V_A has no dependence on V_B . However, V_B represents the binding potential of an electron to a neutral hydrogen atom, and the atom is itself polarized by the applied field. This, then, modifies V_B . Nevertheless, it is very instructive to suppose the independence of V_A and V_B , and see what emerges.

Appendix A gives a derivation of the full S matrix for the case when the particle bound by potential V_B (where V_B is presumed independent of the applied field) is affected by the introduction of the potential V_A . Equation (3) is just the leading term of Eq. (A17) or (A18), with the notational correspondence that Ψ_B of Appendix A is rendered as Φ here. An assessment of the accuracy of the approximation represented by Eq. (3) can be obtained by comparing the magnitude of the second term in Eq. (A18) with the first term. For order-of-magnitude purposes, the theta function in the second term can be ignored, and the integral over t_1 of $(\Psi_{A_j}, V_A \Psi_{B_j})$ can be equated to the integral of $(\Psi_{A_j}, V_A \Psi_{B_j})$ in the leading term. The ratio of the magnitude of the second term to the first is then to be found by estimating the magnitude of

$$\int dt_2 (\Psi_f^{(-)}, V_B \Psi_{A_j})_{t_2}.$$

The state $\Psi_f^{(-)}$ can, from Eq. (A10), be approximated by Ψ_{A_j} . The integral to consider is then

$$\int dt_2 (\Psi_{A_j}, V_B \Psi_{A_j})_{t_2}. \quad (4)$$

Were the factor V_B not present in the inner pro-

duct in Eq. (4), it would be just an orthonormality expression for the Ψ_A states, with a value of unity. The presence of V_B in the inner product affects its value in two basic ways. Consider the inner product to be in configuration representation, so it is a spatial integral. First, since V_B represents the binding potential, and since Ψ_A is just a modulated plane wave of essentially uniform magnitude over the volume of integration, then the magnitude E_B can be extracted from the inner product, where E_B is the binding energy. Second, V_B is taken to be a finite-range potential which affects a volume much smaller than that encompassed by the applied field. The inner product in Eq. (4) will then be taken to be of order

$$(\Psi_{A_j}, V_B \Psi_{A_j}) = O(E_B R_0^3 / N \lambda^3),$$

where R_0 is the range of the potential V_B , and the state Ψ_A (in configuration representation) is taken to be normalized over a volume whose transverse dimensions must be at least λ (the wavelength of the field), and whose extent in the direction of propagation of the field is N wavelengths. The binding energy is of order

$$E_B = O(1/mR_0^2),$$

which is generally true for atomic and molecular problems.¹² The time integration in Eq. (4) is nominally between infinite limits, but if the field is N wavelengths in spatial extent it is N periods in temporal extent so

$$\begin{aligned} \int dt_2 |(\Psi_{A_j}, V_B \Psi_{A_j})_{t_2}| &= O\left(\frac{1}{mR_0^2} \frac{R_0^3}{N \lambda^3} N \lambda\right) \\ &= O\left(\frac{\lambda_c R_0}{\lambda \lambda}\right), \end{aligned} \quad (5)$$

where $\lambda_c (=1/m)$ is the electron Compton wavelength. For λ of about 10^{-3} cm and R_0 of the order of angstroms, the right-hand side of Eq. (5) is roughly 10^{-12} . This represents just one term in the sum over j shown in Eq. (A18), but even if Eq. (5) is multiplied by the number of modes in the field, the result will still be small.

In the physical justification given at the beginning of this section for adopting Eq. (3) as an approximate S matrix, the notion of high field intensity was used. In arriving at the error estimate of Eq. (5), however, the essential point was the limited range of V_B , and the field intensity does not appear at all. In fact, it will be shown later that the results derived from Eq. (3) reduce to the expected limit when the field intensity becomes small.

As discussed in Appendix A, the complete S matrix can be developed in a perturbation expan-

sion either in terms of V_A or V_B . Equation (3) and the error estimates just given apply to the leading term in an expansion in V_B . Had an expansion in V_A been adopted instead, Eq. (A15) would apply. An order-of-magnitude analysis of the type just given, when applied to a comparison of the second term in Eq. (A15) with the leading term, leads to a result which is dependent on field intensity, and will be small only when the intensity is low. The approach based on Eq. (3) is thus much more suitable than one based on Eq. (A15).

An important point can be made about the effect of the field on V_B . The error estimate based on Eq. (5) refers to the error incurred in using Eq. (3) as an approximation to Eq. (2); it refers to the error involved in neglecting the effect of the finite-range binding potential on the unbound final state. In the above discussion, V_B is assumed to be independent of \vec{A} . When V_B is modified due to effects of the applied field, the qualitative remarks stemming from Eq. (5) remain unchanged as long as V_B is not converted by the field from a short-range to a long-range potential.

III. TRANSITION PROBABILITY

A. General wave-packet S matrix

The S matrix to be calculated is given in Eq. (3), where the state vectors Ψ_A and Φ , and the operator V_A are now to be used in configuration representation. The applied electromagnetic field will be treated in radiation gauge, so that

$$V_A(t) = -\frac{e\vec{A} \cdot (-i\vec{\nabla})}{m} + \frac{e^2 A^2}{2m}. \quad (6)$$

$$(S-1)_{fi} = -i \left(\frac{e^{i\vec{p} \cdot \vec{r}}}{V^{1/2}}, \phi_i(\vec{r}) \right) \int_{-\infty}^{\infty} dt e^{i\phi^2/2m-E} t V_A(\vec{p}, t) \exp \left(i \int_{-\infty}^t d\tau V_A(\vec{p}, \tau) \right). \quad (11)$$

An integration by parts can now be carried out in the integral over t . This leads to an integrated part to be evaluated at $t = \pm\infty$. However, for periodic \vec{A} , the expression

$$\lim_{t \rightarrow \pm\infty} \left[e^{i\phi^2/2m-E} t \exp \left(i \int_{-\infty}^t d\tau V_A(\vec{p}, \tau) \right) \right]$$

is just the zero distribution, and so the integration by parts gives

$$(S-1)_{fi} = \frac{i}{V^{1/2}} \hat{\phi}_i(\vec{p}) \left(\frac{p^2}{2m} - E_i \right) \int_{-\infty}^{\infty} dt e^{i\phi^2/2m-E} t \exp \left(i \int_{-\infty}^t d\tau V_A(\vec{p}, \tau) \right), \quad (12)$$

where $\hat{\phi}_i(\vec{p})$ is the Fourier transform of $\phi_i(\vec{r})$,

$$\hat{\phi}_i(\vec{p}) = \int d^3r e^{-i\vec{p} \cdot \vec{r}} \phi_i(\vec{r}). \quad (13)$$

Equation (12) is the basic expression from which transition probabilities will be calculated. The electromagnetic field enters in the exponential of

The advantages of radiation gauge for intense-field problems are described in Ref. 6. Furthermore, the use of radiation gauge leads to an analytical simplicity which confers major benefits which will become evident below. Some of these benefits have already been demonstrated in a treatment of intense-field induced interband transitions in solids.⁵ The wave functions Ψ_A are the long-wavelength-approximation Volkov solutions in radiation gauge

$$\Psi_A = \frac{1}{V^{1/2}} \exp \left(i\vec{p} \cdot \vec{r} - i \frac{p^2}{2m} t - i \int_{-\infty}^t d\tau V_A(\vec{p}, \tau) \right), \quad (7)$$

where $V_A(\vec{p}, t)$ is given by Eq. (6) with the $-i\vec{\nabla}$ operator replaced by the eigenvalue \vec{p} , and where V is a normalization volume. Note that Ψ_A is an eigenfunction¹³ of the $V_A(t)$ operator,

$$V_A(t)\Psi_A = V_A(\vec{p}, t)\Psi_A. \quad (8)$$

The initial-state wave function Φ_i is a stationary bound state,

$$\Phi_i(\vec{r}, t) = \phi_i(\vec{r}) e^{-iE_i t}. \quad (9)$$

Since V_A is a Hermitian operator, the S -matrix expression in Eq. (3) can be written with the help of Eq. (8) as

$$(S-1)_{fi} = -i \int_{-\infty}^{\infty} dt (V_A \Psi_A, \Phi_i)_t \\ = -i \int_{-\infty}^{\infty} dt V_A(\vec{p}, t) (\Psi_A, \Phi_i)_t. \quad (10)$$

With Eqs. (7) and (9) employed in (10), the result is

the integrand in the $V_A(\vec{p}, \tau)$ factor. In principle, the field can be any wave packet which vanishes at infinite times, subject to the limitations that the frequency components of the packet must all propagate in the same direction and must satisfy the long-wavelength approximation. The initial bound state enters in Eq. (12) only through its momentum-space wave function $\hat{\phi}_i(\vec{p})$.

B. Transition probability for circular polarization

The S matrix will now be written for the case of a monochromatic circularly polarized plane wave. The word "monochromatic" must be qualified to the extent that the electromagnetic field is presumed to be adiabatically turned off at $|t| \rightarrow \infty$. The vector potential in long-wavelength approximation for circular polarization is

$$\vec{A} = \frac{1}{2}a(\vec{\epsilon}e^{i\omega t} + \vec{\epsilon}^*e^{-i\omega t}), \quad (14)$$

with

$$\vec{\epsilon}^2 = \vec{\epsilon}^*{}^2 = 0, \quad \vec{\epsilon} \cdot \vec{\epsilon}^* = 1. \quad (15)$$

The Volkov wave function (7) is then

$$\psi_A = V^{1/2} \exp\left(i\vec{p} \cdot \vec{r} - i\frac{p^2}{2m}t - iz\omega t + i\zeta_c \sin(\omega t - \varphi)\right), \quad (16)$$

where z is a fundamental intensity parameter¹⁴ defined by

$$z = e^2 d^2 / 4m\omega, \quad (17)$$

ζ_c is the intensity-dependent amplitude

$$\zeta_c = ea|\vec{p} \cdot \vec{\epsilon}|/m\omega, \quad (18)$$

$$(S-1)_{fi} = \frac{i}{V^{1/2}} \hat{\phi}_i(\vec{p}) \left(\frac{p^2}{2m} - E_i\right) \int_{-\infty}^{\infty} dt \exp\left[i\left(\frac{p^2}{2m} - E_i + z\omega\right)t - i\zeta_c \sin(\omega t \mp \varphi)\right]. \quad (24)$$

The use of the generating function for the Bessel function

$$\exp[-i\zeta_c \sin(\omega t \mp \varphi)] = \sum_{n=-\infty}^{\infty} J_n(\zeta_c) e^{-in(\omega t \mp \varphi)}, \quad (25)$$

puts the integral over t in Eq. (24) in the form of a representation of the delta function, so Eq. (24) is

$$(S-1)_{fi} = \frac{2\pi i}{V^{1/2}} \hat{\phi}_i(\vec{p}) \sum_n (n\omega - z\omega) e^{in\varphi} J_n(\zeta_c) \times \delta\left(\frac{p^2}{2m} - E_i - n\omega + z\omega\right). \quad (26)$$

The transition probability per unit time, w , is found from

$$w = \lim_{t \rightarrow \infty} \frac{1}{t} |(S-1)_{fi}|^2. \quad (27)$$

The delta functions in Eq. (26) cause incoherence between contributions from different terms in the sum over n . The result of the operations indicated in Eq. (27) is

and φ is the phase angle of $\vec{\epsilon}$ with respect to \vec{p} ,

$$\vec{p} \cdot \vec{\epsilon} = |\vec{p} \cdot \vec{\epsilon}| e^{-i\varphi}. \quad (19)$$

For example, if the electromagnetic wave propagates in the direction of the z axis, then the polarization vector is

$$\vec{\epsilon} = 2^{-1/2}(\hat{e}_x \mp i\hat{e}_y), \quad (20)$$

where \hat{e}_x, \hat{e}_y are unit vectors along the x and y axes, respectively, and the upper and lower signs in Eq. (20) refer to right and left circular polarization, respectively. Equation (19) can then be written as

$$\vec{p} \cdot \vec{\epsilon} = 2^{-1/2}(p_x \mp ip_y) = 2^{-1/2}p_\perp \exp(\mp i \arctan p_y/p_x). \quad (21)$$

That is, p_\perp is the component of momentum transverse to the direction of propagation of the field

$$p_\perp = 2^{1/2}|\vec{p} \cdot \vec{\epsilon}| = |p_x \mp ip_y|, \quad (22)$$

and the phase angle is

$$\varphi = \arctan p_y/p_x. \quad (23)$$

In terms of the above notation, Eq. (12) is

$$w = \frac{2\pi}{V} |\hat{\phi}_i(\vec{p})|^2 \omega^2 \sum_n (n-z)^2 |J_n(z^{1/2}\gamma)|^2 \times \delta\left(\frac{p^2}{2m} - E_i - n\omega + z\omega\right), \quad (28)$$

where the ζ_c parameter of Eq. (18) is now rendered as

$$\zeta_c = z^{1/2}\gamma, \quad \gamma = (2/m\omega)^{1/2} p \sin\theta. \quad (29)$$

The purpose of this new definition is to exhibit explicitly the intensity dependence of ζ_c . The angle θ which appears in Eq. (29) is with respect to an axis of spherical polar coordinates, where $p = |\vec{p}|$. In other words, $p \sin\theta$ is just p_\perp of Eq. (22).

The total transition probability is found from integrating w over all final states available to the detached particle. The Volkov states are continuum states with momentum parameter p . The total transition probability, W , is thus

$$W = \int \frac{V d^3 p}{(2\pi)^3} w, \quad (30)$$

$$= \frac{1}{(2\pi)^3} \int V p^2 dp d\Omega w,$$

where $(2\pi)^3$ is the size of a unit volume in phase space, and $d\Omega$ is the differential solid angle. With Eq. (28) employed in (30), the differential form of the total transition probability per unit time is

$$\frac{dW}{d\Omega} = \frac{\omega^2}{(2\pi)^2} \sum_n (n-z)^2 \int p^2 dp |\hat{\phi}_i(\vec{p})|^2 J_n^2(z^{1/2}\gamma) \times \delta\left(\frac{p^2}{2m} - E_i - n\omega + z\omega\right). \quad (31)$$

The delta function in Eq. (31) can be used to accomplish the integral over p . The delta function is in terms of p^2 , but it is made directly usable for positive values of p by writing

$$\delta\left(\frac{p^2}{2m} + E_B - n\omega + z\omega\right) = (m/2\omega)^{1/2} (n-z - E_B/\omega)^{-1/2} \times \delta[p - (2m\omega)^{1/2} (n-z - E_B/\omega)^{1/2}].$$

In this expression, the bound-state nature of the initial state ($E_i < 0$) is made manifest by setting

$$E_B = -E_i,$$

where E_B is the (positive) binding energy. The integrated form of Eq. (31) is

$$\frac{dW}{d\Omega} = \frac{(2m^3\omega^5)^{1/2}}{(2\pi)^2} \sum_n (n-z)^2 (n-z - \epsilon_B)^{1/2} \times |\hat{\phi}_i(\vec{p})|^2 J_n^2(z^{1/2}\gamma), \quad (32)$$

where the notation $\epsilon_B \equiv E_B/\omega$ has been introduced. It is important to keep in mind that the p which appears in γ [as given by Eq. (29) and in $|\hat{\phi}_i(\vec{p})|^2$] is to be replaced by the value arising from the delta function, which is

$$p = (2m\omega)^{1/2} (n-z - \epsilon_B)^{1/2}. \quad (33)$$

This means that $|\hat{\phi}_i(\vec{p})|^2$ depends on n , z , E_B , and ω , in general. The new form of γ is

$$\gamma = 2(n-z - \epsilon_B)^{1/2} \sin\theta. \quad (34)$$

Equation (32) is the final form of the differential total transition probability per unit time for photodetachment arising from monochromatic circularly polarized electromagnetic fields. It is a closed-form analytical expression as long as there is an analytical form for the initial-state wave function in momentum representation. The physical content of the conservation condition, Eq. (33), is perhaps most easily seen in the quadratic form

$$p^2/2m = (n-z - \epsilon_B)\omega. \quad (35)$$

First, consider Eq. (35) in the low-intensity limit, $z \rightarrow 0$. Equation (35) then says that the final kinetic

energy of the photodetached electron is given by the energy contributed by an n th order interaction with the field (loosely speaking, the energy of n photons, $n\omega$), less the energy which must be invested in overcoming the initial binding energy of the electron, E_B . In the general case, where $z \neq 0$, the energy $z\omega$ is a minimal interaction energy of the charged particle with the electromagnetic field.

A consequence of Eqs. (33) or (35) is that n is bounded from below, since

$$n \geq z + \epsilon_B. \quad (36)$$

In terms of integer relationships,

$$n \geq n_0, \quad (37)$$

$$n_0 \equiv [z + \epsilon_B],$$

where n_0 is the smallest index in the sum over n , and the square bracket in Eq. (37) signifies the smallest integer containing the quantity within the bracket. The range of n , initially [Eq. (25)] $-\infty < n < \infty$, is now confined to $n_0 \leq n < \infty$.

C. Transition probability for linear polarization

The vector potential for a monochromatic linearly polarized plane wave in long-wavelength approximation is

$$\vec{A} = a\vec{\epsilon} \cos\omega t,$$

where $\vec{\epsilon}$ is real and normalized ($\vec{\epsilon}^2 = 1$), and an adiabatic cutoff of \vec{A} at $|t| \rightarrow \infty$ is understood. The Volkov wave function is

$$\Psi_A = V^{-1/2} \exp\left(i\vec{p} \cdot \vec{r} - i\frac{p^2}{2m}t - iz\omega t + i\zeta_i \sin\omega t - i\frac{z}{2} \sin 2\omega t\right), \quad (38)$$

where z is defined in Eq. (17) and ζ_i is the real intensity-dependent amplitude

$$\zeta_i \equiv ea\vec{p} \cdot \vec{\epsilon}/m\omega. \quad (39)$$

The S matrix, as given by Eq. (12), becomes

$$(S-1)_{fi} = \frac{i}{V^{1/2}} \hat{\phi}_i(\vec{p}) \left(\frac{p^2}{2m} - E_i\right) \times \int_{-\infty}^{\infty} dt \exp\left[i\left(\frac{p^2}{2m} - E_i + z\omega\right)t - i\zeta_i \sin\omega t + \frac{iz}{2} \sin 2\omega t\right]. \quad (40)$$

At this point it is appropriate to introduce a generalized Bessel function $J_n(u, v)$, whose definition and principal properties are given in Appendix B. The generating function for $J_n(u, v)$, given in Eq. (B11), leads to the expression

$$\exp\left(-i\zeta_i \sin\omega t + i\frac{z}{2} \sin 2\omega t\right) = \sum_{n=-\infty}^{\infty} J_n\left(\zeta_i, -\frac{z}{2}\right) e^{-in\omega t} \quad (41)$$

when Eq. (B7) is used. Equation (40) can now be written

$$(S-1)_{fi} = \frac{2\pi i}{V^{1/2}} \hat{\phi}_i(\vec{p}) \sum_n (n\omega - z\omega) J_n\left(\zeta_i, -\frac{z}{2}\right) \times \delta\left(\frac{p^2}{2m} - E_i - n\omega + z\omega\right), \quad (42)$$

in close analogy to Eq. (26).

The transition probability per unit time, found by using Eq. (42) in Eq. (27), is

$$w = \frac{2\pi}{V} |\hat{\phi}_i(\vec{p})|^2 \omega^2 \sum_n (n-z)^2 \left| J_n\left(z^{1/2}\alpha, -\frac{z}{2}\right) \right|^2 \times \delta\left(\frac{p^2}{2m} - E_i - n\omega + z\omega\right), \quad (43)$$

where the intensity dependence of the ζ_i parameter is made manifest by the notation

$$\zeta_i = z^{1/2}\alpha, \quad (44)$$

$$\alpha = 2(m\omega)^{-1/2} p \cos\theta.$$

The angle θ is the polar angle in spherical polar coordinates, but in this linear polarization case, the polar axis is taken to be along the polarization vector, $\vec{\epsilon}$. Thus, the spherical polar coordinates are oriented differently in the circular and linear polarization cases.

The total transition probability per unit time, Eq. (30), leads to

$$\frac{dW}{d\Omega} = \frac{(2m^3\omega^5)^{1/2}}{(2\pi)^2} \sum_{n=n_0}^{\infty} (n-z)^2 (n-z-\epsilon_B)^{1/2} \times |\hat{\phi}_i(\vec{p})|^2 J_n^2\left(z^{1/2}\alpha, -\frac{z}{2}\right) \quad (45)$$

by the same sequence of steps which led to the very similar Eq. (32) for circular polarization. As before, the p which appears in α and in $|\hat{\phi}_i(\vec{p})|^2$, is given in Eq. (33), and α can now be expressed as

$$\alpha = 8^{1/2} (n-z-\epsilon_B)^{1/2} \cos\theta. \quad (46)$$

As in the circular polarization case, $dW/d\Omega$ for linear polarization as given by Eq. (45) is an entirely analytic expression as long as an analytic form exists for the momentum-space initial wave function. An important difference in the two cases is the occurrence of the generalized Bessel function $J_n(z^{1/2}\alpha, -\frac{1}{2}z)$ in Eq. (45). This gives a much more complicated structure to the linear polarization case. For one thing, it introduces

very different behavior for even and odd values of n , as can be seen by observing some of the properties of $J_n(u, v)$ given in Appendix B.

D. Limitations

It has been stressed that Eqs. (32) and (45) are closed analytical forms obtained without the need for any approximations beyond those inherent in using Eq. (3). As indicated in the discussion in Sec. II, a finite range for the binding potential V_B should be enough to assure the accuracy of Eq. (3). Other limitations do exist, however, which will be noted here.

The order of magnitude analysis associated with Eq. (5) takes no account of the possibility of intermediate resonances associated with the binding potential. Suppose, for example, the cautions about a long-range potential (like the Coulomb potential) were ignored, and the above formalism was applied to photoionization of a neutral atom from the ground state. If energy conservation demands a multiphoton process, then there is a possibility that some number of photons less than the threshold number for ionization will be resonant with an excited bound state. Ionization then takes place in two stages—excitation, followed by ionization from the excited state. When such a resonance is possible, it becomes the dominant mode of ionization. The analysis connected with Eq. (5), and the conclusions therefrom, are not valid if such a resonance can occur with a bound excited state.

Another caution which must be observed has to do with depletion effects, which can occur when W is of the order of $(\Delta t)^{-1}$, where Δt is the duration of the electromagnetic pulse. For the sake of simple exposition, consider a square pulse of radiation turned on at time $t=0$. If N_0 is the initial number of particles in the target region which are candidates for photodetachment, then at time t ($t < \Delta t$), the number remaining is

$$N = N_0 e^{-Wt},$$

and the yield of photodetached electrons expressed as a fraction of the initial particles present is

$$Y = (N_0 - N)/N_0 = 1 - e^{-Wt}. \quad (47)$$

Thus, if $W\Delta t \ll 1$, the yield builds linearly with time

$$Y \approx Wt \quad (W\Delta t \ll 1),$$

permitting direct experimental determination of W by measuring $W\Delta t$. If however, $W\Delta t \gg 1$, then Eq. (47) shows that $Y \rightarrow 1$ before the pulse is finished, and W cannot be determined from the total yield. (This assumes that time resolution of Y

during the pulse is not possible.) It will be assumed hereafter that only

$$W \ll 1/\Delta t \quad (48)$$

will be of interest. If Δt as short as 10^{-12} sec is considered for $1.06\text{-}\mu\text{m}$ radiation, then W as large as perhaps 10^{11} sec^{-1} can be treated. For $10.6\text{-}\mu\text{m}$ radiation, $\Delta t \sim 5 \times 10^{-11}$ sec is currently appropriate, so W as large as 2×10^9 is of interest.

If the yield of photoelectrons during a pulse could be time resolved, then another limitation would have to be considered. The formalism used above for finding W makes use of a large-time limiting procedure. Were saturation of the transition probability to occur during a time of the order of a single wave period, the above formalism for W is not applicable. To use the present formalism, the constraint

$$W \ll 1/T, \quad (49)$$

is required (T is the wave period), which allows consideration of much larger W than does Eq. (48). The condition (49) will be examined in more detail in Sec. VI.

As discussed in Sec. II, the presumption is made that V_B does not experience a major alteration as a consequence of the application of the external field.

Subject to the limitations (48) and (49), and the cautions about intermediate multiphoton resonances and field-independence of V_B , Eqs. (32) and (45) are intense-field expressions which can describe n th order processes in a single closed-form ex-

pression. They are not limited by convergence constraints on intensity as is perturbation theory. The convergence of perturbation theory is examined in Sec. IX.

IV. LOW-INTENSITY LIMIT

A. Circular polarization

The differential transition probability for the case of circular polarization when the field intensity is low is found readily from Eq. (32). Because the argument of the Bessel function is small when z is small, the lowest-order Bessel function will be dominant, and only the $n = n_0$ term in the sum needs to be retained. With the approximation

$$J_{n_0}^2(z^{1/2}\gamma) \approx (n_0!)^{-2} z^{n_0} (n_0 - \epsilon_B)^{n_0} \sin^{2n_0}\theta,$$

which follows from Eq. (34) for γ , $dW/d\Omega$ for circular polarization is

$$\frac{dW}{d\Omega} \approx \frac{(2m^3\omega^5)^{1/2} (n_0 - \epsilon_B)^{n_0+1/2}}{(2\pi)^2 [(n_0 - 1)!]^2} |\hat{\phi}_i(\vec{p})|^2 z^{n_0} \sin^{2n_0}\theta \quad (50)$$

for low field intensity. In the special case that $|\hat{\phi}_i(\vec{p})|^2$ is independent of the θ , φ angular coordinates, the differential transition probability in Eq. (50) can be integrated over solid angle. The momentum-space initial-state wave function will be independent of angular coordinates if the configuration-space wave function $\phi_i(\vec{r})$ is a function of r only. If such is the case, integration over the solid angle gives

$$W \approx \frac{(2m^3\omega^5)^{1/2}}{\pi} \frac{2^{2n_0} n_0^2 (n_0 - \epsilon_B)^{n_0+1/2}}{(2n_0 + 1)!} |\hat{\phi}_i(\vec{p})|^2 z^{n_0}. \quad (51)$$

B. Linear polarization

Low-intensity results for linear polarization are more complicated than the circular case because of the presence of the generalized Bessel functions in Eq. (45). It is shown in Appendix C that $J_n(z^{1/2}\alpha, -\frac{1}{2}z)$ behaves as $z^{n/2}$ for small z , so again the sum over n reduces to the leading term, $n = n_0$. For even n_0 , Eqs. (C2) and (46) give the result

$$J_{n_0}\left(z^{1/2}\alpha, -\frac{z}{2}\right) \approx \left(-\frac{z}{4}\right)^{n_0/2} \sum_{k=0}^{n_0/2} \frac{(-8)^k (n_0 - \epsilon_B)^k \cos^{2k}\theta}{(2k)! (n_0/2 - k)!}.$$

This leads to

$$\frac{dW}{d\Omega} = \frac{(2m^3\omega^5)^{1/2}}{(2\pi)^2} n_0^2 (n_0 - \epsilon_B)^{1/2} |\hat{\phi}_i(\vec{p})|^2 \left(\frac{z}{4}\right)^{n_0} \sum_{k=0}^{n_0/2} \sum_{l=0}^{n_0/2} \frac{(-8)^{k+l} (n_0 - \epsilon_B)^{k+l} \cos^{2(k+l)}\theta}{(2k)! (2l)! (\frac{1}{2}n_0 - k)! (\frac{1}{2}n_0 - l)!}, \quad (52)$$

and, if $|\hat{\phi}_i(\vec{p})|^2$ is independent of angular coordinates,

$$W = \frac{(2m^3\omega^5)^{1/2}}{\pi} n_0^2 (n_0 - \epsilon_B)^{1/2} |\hat{\phi}_i(\vec{p})|^2 \left(\frac{z}{4}\right)^{n_0} \sum_{k=0}^{n_0/2} \sum_{l=0}^{n_0/2} \frac{(-8)^{k+l} (n_0 - \epsilon_B)^{k+l}}{(2k)! (2l)! (\frac{1}{2}n_0 - k)! (\frac{1}{2}n_0 - l)! (2k + 2l + 1)}. \quad (53)$$

For odd n_0 , Eqs. (C3) and (46) yield

$$J_{n_0}\left(z^{1/2}\alpha, -\frac{z}{2}\right) \approx (-)^{(n_0+1)/2} 8^{1/2} \left(\frac{z}{4}\right)^{n_0/2} \sum_{k=0}^{(n_0-1)/2} \frac{(-8)^k (n_0 - \epsilon_B)^{k+1/2} \cos^{2k+1}\theta}{(2k+1)! [(n_0-1)/2 - k]!},$$

which gives the results

$$\frac{dW}{d\Omega} \approx \frac{8(2m^3\omega^5)^{1/2}}{(2\pi)^2} n_0^2 (n_0 - \epsilon_B)^{3/2} |\hat{\phi}_i(\vec{p})|^2 \left(\frac{z}{4}\right)^{n_0} \sum_{k=0}^{(n_0-1)/2} \sum_{l=0}^{(n_0-1)/2} \frac{(-8)^k (n_0 - \epsilon_B)^{k+l} \cos^{2k+l}\theta}{(2k+1)!(2l+1)! \left[\frac{1}{2}(n_0-1)-k\right]! \left[\frac{1}{2}(n_0-1)-l\right]!}, \quad (54)$$

and, when $|\hat{\phi}_i(\vec{p})|^2$ does not depend on θ, φ ,

$$W \approx \frac{8(2m^3\omega^5)^{1/2}}{\pi} n_0^2 (n_0 - \epsilon_B)^{3/2} |\hat{\phi}_i(\vec{p})|^2 \left(\frac{z}{4}\right)^{n_0} \times \sum_{k=0}^{(n_0-1)/2} \sum_{l=0}^{(n_0-1)/2} \frac{(-8)^{k+l} (n_0 - \epsilon_B)^{k+l}}{(2k+1)!(2l+1)! \left[\frac{1}{2}(n_0-1)-k\right]! \left[\frac{1}{2}(n_0-1)-l\right]! (2k+2l+3)}. \quad (55)$$

C. First-order processes

A case of special interest is the low-intensity limit for $n_0=1$, since that corresponds to the customary first-order perturbation result. Both Eq. (51) for circular polarization and Eq. (55) for linear polarization reduce to

$$W \approx 2(3\pi)^{-1} (2m^3)^{1/2} \omega (\omega - E_B)^{3/2} |\hat{\phi}_i(\vec{p})|^2 z \quad (56)$$

for $n_0=1$. There are differences, of course, in the angular distributions, with Eq. (50) for circular polarization leading to

$$\frac{dW}{d\Omega} \approx (2\pi)^{-2} (2m^3)^{1/2} \omega (\omega - E_B)^{3/2} |\hat{\phi}_i(\vec{p})|^2 z \sin^2\theta, \quad (57)$$

and Eq. (54) for linear polarization giving

$$\frac{dW}{d\Omega} \approx 2(2\pi)^{-2} (2m^3)^{1/2} \omega (\omega - E_B)^{3/2} |\hat{\phi}_i(\vec{p})|^2 z \cos^2\theta. \quad (58)$$

When $n_0=1$, it is convenient to introduce the notion of differential cross section, $d\sigma/d\Omega$, or total cross section, σ . To go from total transition probability per unit time to cross section, it is necessary to divide by the flux of incoming photons. In the units used here, the photon flux is

$$\text{flux} = \frac{1}{2} a^2 \omega = m\omega^2 z / 2\pi\alpha_0, \quad (59)$$

where α_0 is the fine-structure constant. Thus the total cross section found from Eq. (56) is

$$\sigma = 4\alpha_0 (3\omega)^{-1} (2m)^{1/2} (\omega - E_B)^{3/2} |\hat{\phi}_i(\vec{p})|^2. \quad (60)$$

Low-intensity cross section expressions for $n_0=1$ are independent of the intensity parameter z . That does not remain true for higher orders,

where σ or $d\sigma/d\Omega$ depend on z^{n_0-1} . Total transition probability is a more convenient concept than cross section for high-order processes.

D. Comparison of circular and linear polarization results

A comparison is now made for total transition probability per unit time as brought about by circularly vis-a-vis linearly polarized fields. This is done for arbitrary order, n_0 , but the comparison is confined to the case where the solid-angle integration can be performed in general. That is, the ratio of Eq. (51) to Eq. (53), or Eq. (51) to Eq. (55) is examined.

Considerable interest in comparisons of this sort was sparked several years ago, when experimental results^{15,16} for second- and third-order photoionization of alkali atoms showed circular polarization to be more effective. This was in conformity with prior theoretical predictions by Hernandez and Gold¹⁷ and subsequent work by Lambropoulos,¹⁸ but it appeared to contradict earlier theoretical results of Perelomov, Popov, and Terent'ev,¹⁹ who concluded that linear polarization should be more effective in causing ionization. This situation was clarified by Reiss¹⁰ and by Gontier and Trahin,²⁰ who showed that linear polarization was increasingly more effective than circular polarization as the order of the process increased, but that for second- and third-order processes, circular polarization could indeed be more important.

In the present problem, the ratio of circular to linear transition probabilities in the low-intensity case (when transition probabilities vary as z^{n_0}) is found from the ratio of Eq. (51) to Eq. (53) to be

$$\left(\frac{W_{\text{circ}}}{W_{\text{lin}}}\right)_{n_0 \text{ even}} = \frac{2^{4n_0} (n_0 - \epsilon_B)^{n_0}}{(2n_0 + 1)!} \left(\sum_{k=0}^{n_0/2} \sum_{l=0}^{n_0/2} \frac{[-8(n_0 - \epsilon_B)]^{k+l}}{(2k)!(2l)!(\frac{1}{2}n - k)!(\frac{1}{2}n - l)!(2k+2l+1)} \right)^{-1}, \quad (61)$$

when n_0 is even. When n_0 is odd, Eqs. (51) and (55) yield the ratio

$$\left(\frac{W_{\text{circ}}}{W_{\text{lin}}}\right)_{n_0 \text{ odd}} = \frac{2^{4n_0} (n_0 - \epsilon_B)^{n_0}}{(2n_0 + 1)!} \times \left(\sum_{k=0}^{(n_0-1)/2} \sum_{l=0}^{(n_0-1)/2} \frac{(-)^{k+l} [8(n_0 - \epsilon_B)]^{k+l+1}}{(2k+1)!(2l+1)! \left[\frac{1}{2}(n_0-1)-k\right]! \left[\frac{1}{2}(n_0-1)-l\right]! (2k+2l+3)} \right)^{-1}. \quad (62)$$

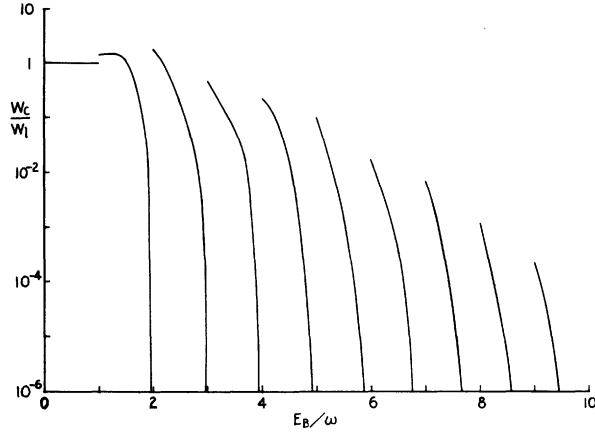


FIG. 1. Transition probability in a circularly polarized field as compared to a linearly polarized field in the low-intensity case. The ratio is plotted against E_B/ω , the binding energy expressed in units of a photon energy.

These results are plotted in Fig. 1.

It is seen that circular and linear polarization transition probabilities are equal for $n_0=1$, as expected, and that circular results can exceed linear only for a range of ϵ_B values within the $n_0=2$ and 3 cases. Generally, as n_0 increases, the ratio $W_{\text{circ}}/W_{\text{lin}}$ declines, but superimposed on this general trend is a succession of discontinuities marking the thresholds for new n_0 values. The maximum value the circular-to-linear ratio can attain in this formalism is 1.5 when $n_0=2$, or 1.9 when $n_0=3$. Results for the maxima of the circular-to-linear ratio derived from perturbation theory treatments of atomic photoionization are 1.5 (Refs. 17, 18) for $n_0=2$, and 2.5 (Ref. 18) for $n_0=3$. The measured values in photoionization of alkali atoms are 1.28 ± 0.2 (Ref. 15) for $n_0=2$, and 2.15 ± 0.4 (Ref. 16) for $n_0=3$.

V. HIGH-INTENSITY LIMIT

A. Circular polarization

The high-intensity ($z \gg 1$) limit for the case of circular polarization is found in a very straightforward way by using the appropriate asymptotic form of the Bessel functions which appear in the $dW/d\Omega$ expression in Eq. (32). The essential starting point in choosing the correct asymptotic form is to determine the relative orders of magnitude of the order, n , and argument, $z^{1/2}\gamma$, of the Bessel function. Equation (34) for γ , and Eqs. (36) and (37) for n, z are the essential inputs. Starting from $(n-2z)^2 \geq 0$, which gives $n^2 \geq 4z(n-z)$, it follows that

$$n \geq 2z^{1/2}(n-z)^{1/2} > 2z^{1/2}(n-z-\epsilon_B)^{1/2} \geq z^{1/2}\gamma. \quad (63)$$

The result (63), showing the order of the Bessel function to always exceed the argument, points to the asymptotic form

$$J_n(z^{1/2}\gamma) \approx (n!)^{-1} (\frac{1}{2}z^{1/2}\gamma)^n. \quad (64)$$

When substituted in Eq. (32), Eq. (64) gives

$$\frac{dW}{d\Omega} \approx \frac{(2m^3\omega^5)^{1/2}}{(2\pi)^2} \sum_{n=n_0}^{\infty} \frac{(n-z)^2(n-n_0)^{n+1/2}}{(n!)^2} z^n \times |\hat{\phi}_i(\vec{p})|^2 \sin^2\theta, \quad (65)$$

since it is justifiable in view of the large values for z and n_0 to ignore the bracket in Eq. (37), and simply set $n_0 = z + \epsilon_B$. The large value for n_0 associated with $z \gg 1$ also predicts a very sharp peak in the differential transition probability at $\theta \approx \pi/2$.

In the special case that $\phi_i(\vec{r})$ has spherical symmetry, so that $\hat{\phi}_i(\vec{p})$ is independent of angular coordinates, the solid-angle integration in Eq. (65) can be performed, which leads to

$$W \approx \frac{(2m^3\omega^5)^{1/2}}{\pi} \sum_{n=n_0}^{\infty} \frac{(n-z)^2(4z)^n(n-n_0)^{n+1/2}}{(2n+1)!} |\hat{\phi}_i(\vec{p})|^2. \quad (66)$$

B. Linear polarization

Investigation of the high-intensity limit in the linear polarization case is complicated by the multiparameter nature of the generalized Bessel function which appears in Eq. (45). Many different asymptotic forms of $J_n(u, v)$ exist, depending on the relative magnitudes of n, u, v . The form appropriate for the physical problem being explored here is developed in Appendix D. The result given in Eqs. (D11)–(D13) is accurate to within a few percent for $z \geq 10$.

When Eqs. (D11) and (D13) are employed in the expression for the differential transition probability in Eq. (45), the result is of the form

$$\frac{dW}{d\Omega} = \sum_{n=n_0}^{\infty} f(n, z, \epsilon_B, \cos\theta) e^{g(n, z, \epsilon_B, \cos\theta)}, \quad (67)$$

where

$$g(n, z, \epsilon_B, \cos\theta) = RU^{1/2} + 3\alpha(Q-U)^{1/2}/\delta^{1/2} - 2n \operatorname{arcsinh}[(n-3z+Q)/2z]^{1/2}, \quad (68)$$

with symbols as defined in Eqs. (46) and (D12). Since $z \gg 1$ implies $n_0 \gg 1$, the sum over n in Eq. (67) can be treated approximately as an integration over the variable β defined by

$$\beta = (n - n_0)/n_0. \quad (69)$$

Equation (67) then takes the form

$$\frac{dW}{d\Omega} = \int_0^{\infty} d\beta F(\beta, z, \epsilon_B, \cos\theta) e^{G(\beta, z, \epsilon_B, \cos\theta)}. \quad (70)$$

In its most general terms, Eq. (70) is very complicated, and the integration cannot be performed. However, if the exponential in Eq. (70) can be approximated by the first two terms in a Taylor expansion in β , then an approximate integration can be performed easily. The physical circumstances under which this is possible will be shown to correspond to the so-called "tunneling limit," where the binding energy is much in excess of a photon energy of the applied field. That is, the inequality $\epsilon_B \gg 1$ applies.

The power series expansion of the argument of the exponential function in Eq. (70) can be written as

$$G = G_0 + G'_0\beta + \dots, \quad (71)$$

with obvious meanings for G_0 and G'_0 . From Eqs. (68), (69), and (D12) it can be shown that

$$G_0 = -2(z + \epsilon_B) \operatorname{arcsinh}(\epsilon_B/2z)^{1/2} + [\epsilon_B(2z + \epsilon_B)]^{1/2}, \quad (72)$$

$$G'_0 = -2(z + \epsilon_B) \operatorname{arcsinh}(\epsilon_B/2z)^{1/2} + \frac{1}{2}(z + \epsilon_B)[\epsilon_B/(2z + \epsilon_B)]^{1/2} \cos^2\theta. \quad (73)$$

It is convenient to introduce the parameter

$$z_1 \equiv 2z/\epsilon_B = e^2 a^2 / 2mE_B. \quad (74)$$

An upper limit for the value of G'_0 is

$$G'_0 \leq 2z(1 + z_1^{-1})[-\operatorname{arcsinh}z_1^{-1/2} + \frac{1}{4}(1 + z_1)^{-1/2}]. \quad (75)$$

The bracket on the right-hand side of Eq. (75) is negative for all values $z_1 \geq 0.969$. A negative value for G'_0 is a necessary condition to have convergence of the integral in Eq. (70) when only the first two terms in the power series expansion (71) are retained. The effective range of values of β which will contribute is of the order $\Delta\beta \approx |G'_0|^{-1}$, and so the linear term in Eq. (71) would be expected to dominate higher-order terms when G'_0 is negative and $|G'_0| \gg 1$. From Eq. (75) this requires that

$$z_1 \gg 1. \quad (76)$$

The condition (76) justifies an expansion of the $\operatorname{arcsinh}$ function in Eqs. (72) and (73), which gives the results

$$G_0 \approx -8z/3z_1^{3/2}, \quad (77)$$

$$G'_0 \approx -(2z/z_1^{1/2})(1 - \frac{1}{4}\cos^2\theta). \quad (78)$$

The form of G'_0 in Eq. (78) makes possible a more explicit consequence of $|G'_0| \gg 1$ than just $z_1 \gg 1$. It is also required that $z \gg z_1^{1/2}$, or equivalently, it is required that $\epsilon_B^{1/2} \gg (2/z)^{1/2}$. This last inequality is assured by the constraint

$$\epsilon_B \gg 1. \quad (79)$$

When conditions (76) and (79) are satisfied (along with the original requirement $z \gg 1$ employed in Appendix D), Eq. (70) becomes

$$\frac{dW}{d\Omega} \approx e^{\mathcal{E}_0} \int_0^\infty d\beta F e^{-G'_0\beta} \approx e^{G_0} H(z, \epsilon_B, \cos\theta). \quad (80)$$

The form (80), with G_0 given by Eq. (77), is familiar as the form associated with tunneling of a bound particle through a potential barrier when an electric field is imposed. When written in terms of electric field strength as

$$G_0 = -\frac{2}{3}[m(2E_B)^3]^{1/2}/eF, \quad (81)$$

where $F = a\omega$ is the amplitude of the electric field, the exponential has the same form for both constant^{21,22} and time-dependent^{1,19} fields.

C. Intensity parameters

As is evident from the defining relation (74), both quantities z and z_1 are intensity parameters. The z parameter was present from the outset, but z_1 arose only when considering $z \gg 1$ asymptotic forms. The exponential form given in Eqs. (77) or (81) does not hold true generally when $z \gg 1$, but occurs only when the further inequalities $z_1 \gg 1$ and $\epsilon_B \gg 1$ [Eqs. (76) and (79)] are also satisfied. In the work of Keldysh,¹ z is not mentioned at all, and only z_1 is identified as an intensity parameter. The quantity labeled γ by Keldysh is exactly $z_1^{-1/2}$. Keldysh follows quite a different procedure than the one adopted here. He introduces the condition (79) relatively early in his work by employing a steepest-descent calculation based upon ϵ_B as a large parameter. This is done immediately after his Eq. (15). Keldysh then employs the condition (76) to arrive at the analog of Eq. (80) given in his Eq. (20). This means that the general form given in Eq. (45) is bypassed, and thus it is not possible in the Keldysh formalism to explore the general nature of the limits $z \ll 1$ and $z \gg 1$.

As remarked earlier, the intensity parameter z is one of the intensity parameters associated with free-particle interaction with an electromagnetic field. On the other hand, z_1 is a bound-particle intensity parameter. It is not surprising to find both of these types of intensity parameters arising in the present investigation, concerned with photodetachment of a particle initially bound to a short-range potential.

The identification of z_1 as a bound-particle intensity parameter can be made on quite general physical grounds. To assess the intensity of a field, the strength of the field interaction with a bound particle, as expressed by the interaction energy

$e\vec{A} \cdot \vec{p}/m$, can be compared with the binding energy of the particle. The ratio of the two energies has the magnitude

$$\frac{|e\vec{A} \cdot \vec{p}/m|}{E_B} = O\left(\frac{eaR_0E_B}{E_B}\right) = O(eaR_0), \quad (82)$$

where R_0 is a range characteristic of the binding potential. The second statement in Eq. (82) arises from replacement of the \vec{p}/m operator according to the theorem

$$i\vec{p}/m = [\vec{r}, H_0], \quad (83)$$

followed by assessing the magnitude of the commutator in Eq. (83) as it would appear in a transition matrix element. The range R_0 comes from \vec{r} , and E_B is the energy difference between final and initial states as it follows from the difference in the eigenvalues of H_0 when applied to those states. The square of the result given in Eq. (82) gives a general intensity parameter for bound states,

$$z_b = e^2 a^2 R_0^2. \quad (84)$$

Since, for all atomic and molecular problems, the characteristic size of the system is related to the binding energy by¹²

$$R_0^2 \approx 1/mE_B,$$

then Eq. (84) can be written as

$$z_b = e^2 a^2 / mE_B,$$

which is exactly of the form of Eq. (74) for z_1 .

VI. SHORT-TIME BEHAVIOR

The S matrix and transition probability formalism that has been used up to this point has been conventional in the sense that transition amplitudes are calculated by comparing the state of the fully interacting system with a noninteracting system at infinite times. However, a laboratory environment in which very intense fields can be achieved is one in which significant transition probability could occur within times of the order of a single period of the applied plane-wave field. The short-time behavior of the system is now examined in order to determine the conditions under which the infinite-time asymptotic states formalism is meaningful.

Consider a system in which the electromagnetic field is turned on at a finite time t_0 , and the transition amplitude is assessed at a later time t . A transition matrix can be defined either as

$$U_{fi} = (\Phi_f, \Psi_i^{(+)}),$$

analogous to Eq. (A12), or as

$$U_{fi} = (\Psi_f^{(-)}, \Phi_i),_{t_0}, \quad (85)$$

analogous to Eq. (A13) or (1). The procedure that previously led from Eq. (1) to Eq. (11) now leads from Eq. (85) to

$$(U - 1)_{fi} = -i \left(\frac{e^{i\vec{p} \cdot \vec{r}}}{V^{1/2}}, \phi_i(\vec{r}) \right) \int_0^t dt' e^{i(\phi^2/2m + E_B)t'} V_A(\vec{p}, t') \exp\left(i \int_0^{t'} d\tau V_A(\vec{p}, \tau)\right),$$

in which the initial time t_0 has been taken to be $t_0 = 0$, and where $E_B = -E_i > 0$. The integration by parts which formerly gave Eq. (12) now yields

$$(U - 1)_{fi} = \frac{\hat{\phi}_i(\vec{p})}{V^{1/2}} \left[i \left(\frac{p^2}{2m} + E_B \right) \int_0^t dt' e^{i(\phi^2/2m + E_B)t'} \exp\left(i \int_0^{t'} d\tau V_A(\vec{p}, \tau)\right) - e^{i(\phi^2/2m + E_B)t} \exp\left(i \int_0^t d\tau V_A(\vec{p}, \tau)\right) + 1 \right]. \quad (86)$$

A comparison of Eq. (86) with the earlier results in Eq. (12) requires first that the relative importance of the last two terms in the square bracket as compared to the first term be assessed, since only the first term survives in the S matrix. The second element of a comparison is that the significance of the difference in integration limits between the first term in Eq. (86) and the integral in Eq. (12) must be evaluated. For explicitness, this will be done within the context of a monochromatic circularly polarized field. A complete treatment would include wave packet effects, but only orders of magnitude are sought here. Since the zero point of the time coordinate has been fixed as the turn-on time of the field, the time as it appears in the vector potential, Eq. (14), should have a constant phase incorporated in it. Equation (14) is thus replaced by

$$\vec{A} = \frac{1}{2} a (\vec{\epsilon} e^{i\omega(t+\beta)} + \vec{\epsilon}^* e^{-i\omega(t+\beta)}),$$

where β is a constant. After the integration over τ is done, Eq. (86) can be written

$$(U-1)_{fi} = \frac{\hat{\phi}_i(\vec{p})}{V^{1/2}} \exp[i\zeta_c \sin(\omega\beta - \varphi)] \left\{ i \left(\frac{p^2}{2m} + E_B \right) \int_0^t dt' \exp \left[i \left(\frac{p^2}{2m} + E_B + z\omega \right) t' - i\zeta_c \sin(\omega t' + \omega\beta - \varphi) \right] \right. \\ \left. - \exp \left[i \left(\frac{p^2}{2m} + E_B + z\omega \right) t - i\zeta_c \sin(\omega t + \omega\beta - \varphi) \right] \right. \\ \left. + \exp[-i\zeta_c \sin(\omega\beta - \varphi)] \right\}, \quad (87)$$

where the parameters z , ζ_c , and φ are as defined in Eqs. (17)–(19). When an expansion like Eq. (25) is employed for each of the trigonometric functions appearing in an exponential in the brace in Eq. (87), the result is

$$(U-1)_{fi} = \frac{\hat{\phi}_i(\vec{p})}{V^{1/2}} e^{i\zeta_c \sin(\omega\beta - \varphi)} \sum_n J_n(\zeta_c) e^{-in(\omega\beta - \varphi)} \\ \times \left[i \left(\frac{p^2}{2m} + E_B \right) \int_0^t dt' e^{i(p^2/2m + E_B + z\omega)t'} - e^{i(p^2/2m + E_B + z\omega)t} + 1 \right]. \quad (88)$$

Again, it is the first term in the square bracket in Eq. (88) which is to be identified with the S matrix derived earlier. This first term is most important when

$$p^2/2m + E_B + z\omega - n\omega \approx 0, \quad (89)$$

under which condition the first term has a magnitude of approximately $(p^2/2m + E_B)t$. The sum of the second and third terms in the square bracket in Eq. (88) vanish when Eq. (89) has exactly the value zero, and the sum of these two terms is of unit magnitude otherwise. The condition for dominance of the first term is then

$$\omega t \gg \frac{1}{(p^2/2m + E_B)/\omega}. \quad (90)$$

For a process with a multiphoton threshold, the denominator in Eq. (90) has a value greater than unity, and so condition (90) can be stated conservatively as

$$\omega t \gg 1. \quad (91)$$

The next issue to be settled is to identify the set of conditions under which the integral in the first term in the brackets in Eq. (88) acquires the delta-function character imputed to it in the S -matrix formalism. The integral can be stated as

$$\int_0^t dt' e^{i\Delta E t'} = e^{i\Delta E t/2} \left(\frac{\sin \frac{1}{2} \Delta E t}{\frac{1}{2} \Delta E} \right), \quad (92)$$

with the definition of ΔE obvious from a comparison with Eq. (88). A representation of the delta function is

$$\delta(\Delta E) = \frac{1}{2\pi} \lim_{t \rightarrow \infty} \left(\frac{\sin \frac{1}{2} \Delta E t}{\frac{1}{2} \Delta E} \right),$$

and so the question that must be answered is what constitutes a value of t which can be regarded as approaching infinity as far as Eq. (92) is concerned? A graph of Eq. (92) exhibits a sharp peak of

width given by $\frac{1}{2} \Delta E t \approx 1$ in the neighborhood of $t=0$. Delta-function behavior is exhibited when the full peak is encompassed within an energy range $\frac{1}{2} \Delta E \gg \omega$, where ω is the smallest characteristic energy in this physical problem. These two statements combine to exactly the condition given in Eq. (91).

The implication of Eq. (91) is that the formalism developed earlier in this paper is applicable after the field has been on for several full periods. This presumption will be made hereafter. Actually, one could use a finite-time formalism based on Eq. (86) in place of the S -matrix formalism which stems from Eq. (12), but there is no real point in accepting this extra complication. The reason is that another condition will be imposed which makes Eq. (91) irrelevant. It will be required that the total transition probability per unit time be limited to values which do not cause depletion in the target material during a full pulse of the applied field. That is, it will be required that

$$W \ll (\Delta t)^{-1},$$

as given in Eq. (48), where Δt is the pulse duration. The shortest pulses of significance will be taken to be about 10^{-12} sec for $1.06\text{-}\mu\text{m}$ radiation, or 5×10^{-11} sec for $10.6\text{-}\mu\text{m}$ radiation. For a CO_2 laser ($10.6\ \mu\text{m}$), Eq. (48) requires that the transition probability per unit time be limited to much less than 2×10^{10} sec $^{-1}$. The implication of Eq. (91) is that $W \ll \omega$ [see also Eq. (49)] or, for this example of $10.6\text{-}\mu\text{m}$ radiation, W should be much less than 2×10^{14} sec $^{-1}$. The condition (48) is therefore much more stringent than (91), and when Eq. (48) is satisfied, the infinite-time S -matrix formalism is fully justified.

Comments about some results of Geltman^{7,23} are appropriate here. He has found that when an atom is subjected to an oscillatory⁷ or static²³

electric field, the ionization probability does not have a simple exponential time development, but exhibits a plateau phenomenon, with delayed development of exponential behavior. A transition probability per unit time which is independent of time, as is true for the formalism employed here corresponds to exponential time development as shown in Eq. (47). The theoretical framework employed by Geltman is a one-dimensional model atom with a delta-function attractive potential producing a single bound state. Geltman's work, however, is on a very different physical problem than the one considered here. The present problem concerns photodetachment by a plane wave, with emphasis particularly on multiphoton processes. Multiphoton processes require large values of field intensity in order to occur, and such problems are inherently three-dimensional. Specifically, it has been shown⁶ that an intense plane-wave field cannot be approximated as a quasistatic electric field. Even in electric field gauge (or Göppert-Mayer²⁴ gauge), the vector potential of an intense plane wave plays a major role. The direction of this vector potential in electric field gauge is orthogonal to the electric field direction, and it is thus, of necessity, absent in a one-dimensional model. A more physical way to say it is that the magnetic field component of a plane wave becomes very important at high field intensity, but a one-dimensional treatment can describe only the electric field component. Geltman's treatment of the ionization of an atom by an intense electric field thus does not apply to the plane-wave case.

VII. APPLICATION TO H⁻

The negative hydrogen ion is selected as an example with which to illustrate the application of the foregoing formalism. It will be assumed that H⁻ has only one bound state.²⁵ The binding potential is certainly of finite range, in view of the neutrality of the residual atom after photodetachment. Furthermore, a simple analytical approximation for the ground-state wave function of H⁻ has been suggested,⁸ which makes possible the statement of closed analytical forms for $dW/d\Omega$. All of this is advantageous for the application of the present formalism. However, the neutral atom itself can experience excitation and even ionization as a consequence of the applied fields. The interaction of these possibilities with the photodetachment of the excess electron is ignored in the formalism. This may not be a serious limitation on the validity of the results for H⁻. In the numerical application of the present example, the intensity parameter will be limited to

$z=3$ for a 10.6- μm field. This is equivalent to about 3×10^{10} W/cm², which would have only modest effect on a neutral H atom, even though it has very strong effects on the extra electron in H⁻. One way to see this is to note that photodetachment of the extra electron in H⁻ of 0.75-eV binding energy requires a minimum of seven photons when $\lambda=10.6$ μm , whereas excitation of the 10.2-eV first excited state in the neutral H atom requires a minimum of 88 such photons. Another index of the relative ineffectiveness of a 10.6- μm field in perturbing the neutral H atom is that, if the applied field is treated as quasistatic, the resulting second-order Stark effect energy is 4×10^{-6} (measured in rydbergs) at the largest ($z=3$) intensity considered below. All of this suggests the general validity of the results to be obtained despite the neglect of field effects on the neutral atom core of the negative ion.

A. Formalism

The general expressions for the differential transition probability per unit time given in Eqs. (32) and (45) require only the appropriate momentum-space wave function in order to apply to the H⁻ case. The wave function given by Armstrong⁸ is

$$\phi_i(\mathbf{x}) = \frac{\beta^{1/2} f}{(2\pi)^{1/2}} \frac{e^{-\beta r}}{r}, \quad (93)$$

where

$$\beta = (2mE_B)^{1/2}, \quad (94)$$

and f is an empirical constant with the value

$$f^2 = 2.65. \quad (95)$$

The momentum-space wave function that follows from Eqs. (93) and (13) is

$$\hat{\phi}_i(\vec{p}) = 2f(2\pi\beta)^{1/2}/(\beta^2 + p^2). \quad (96)$$

As used in the transition probability, Eq. (96) is to be squared, and the momentum condition arising from the energy delta function, Eq. (33), is to be employed. In other words, the expression needed is

$$[\hat{\phi}_i(\vec{p})]^2 = 8\pi f^2 (2mE_B)^{1/2}/(n-z)^2 (2m\omega)^2. \quad (97)$$

The differential transition probability per unit time for a circularly polarized applied field is, from Eqs. (32) and (97),

$$\frac{dW}{d\Omega} = (f^2/\pi)\omega\epsilon_B^{1/2} \sum_{n=n_0}^{\infty} (n-z-\epsilon_B)^{1/2} J_n^2(z^{1/2}\gamma), \quad (98)$$

where $\epsilon_B = E_B/\omega$, n_0 is defined by Eq. (37), and γ is given in Eq. (34). The corresponding result

for a linearly polarized field is, from Eq. (45),

$$\frac{dW}{d\Omega} = (f^2/\pi)\omega\epsilon_B^{1/2} \sum_{n=n_0}^{\infty} (n-z-\epsilon_B)^{1/2} j_n^2 \left(z^{1/2} \alpha, -\frac{z}{2} \right), \quad (99)$$

with α given in Eq. (46).

B. First-order perturbation limit

The first-order perturbation theory limit of the general theory is found very simply by substitution of Eq. (97) in the low-intensity results given in Sec. IV. For $n_0=1$, the low-intensity form for transition probability per unit time given in Eq. (56) is applicable. The result is simply

$$W = (8/3)f^2 z \omega (1 - \epsilon_B)^{3/2} \epsilon_B^{1/2} \quad (100)$$

for both circular and linear polarization. The corresponding cross section, from Eqs. (60) and (97), or else from Eqs. (59) and (100), is

$$\sigma = (16\pi\alpha_0 f^2 / 3m\omega) (1 - \epsilon_B)^{3/2} \epsilon_B^{1/2}. \quad (101)$$

These limiting results are now to be compared with a direct first-order perturbation calculation of photodetachment based on the ground-state wave function in Eq. (93). The lowest-order final-state wave function is simply the plane wave

$$\phi_f(\vec{r}) = V^{-1/2} \exp(i\vec{p} \cdot \vec{r}). \quad (102)$$

This is consistent with Eq. (7) in lowest order.

The transition matrix element is found by evaluating the first-order term in the interaction Hamiltonian, Eq. (6), between the states given in Eqs. (93) and (102). This gives

$$V_{A_f i}(t) = (\phi_f, m^{-1} e \vec{A} \cdot (-i\vec{\nabla}) \phi_i) = (m^{-1} e \vec{A} \cdot (-i\vec{\nabla}) \phi_f, \phi_i) \\ = (e \vec{A} \cdot \vec{p}/m) (\phi_f, \phi_i), \quad (103)$$

which follows from the hermiticity of $V_A(t)$, and the fact that ϕ_f is an eigenfunction of the momentum operator. When \vec{A} represents a linearly polarized monochromatic plane wave given by

$$\vec{A} = a \vec{\epsilon} \cos \omega t, \quad (104)$$

the space part of Eq. (103) is

$$V_{A_f i} = 4f \left(\frac{2\pi\omega z}{Vm} \right)^{1/2} \frac{(2mE_B)^{1/4} p \cos \theta}{p^2 + 2mE_B}, \quad (105)$$

where θ is the angle between the momentum vector \vec{p} and the polarization vector of the field. The "golden rule" must be written in the form²⁶

$$w = (\pi/2) |V_{A_f i}|^2 \delta(E_f - E_i - \omega), \quad (106)$$

where only the delta function associated with absorption of energy from the field is retained, and the usual golden rule factor of 2π is replaced by $\pi/2$ because each Fourier component in Eq. (104)

has a factor of $\frac{1}{2}$ associated with it. As before, $E_i = -E_B$. The total transition probability per unit time is found by substituting Eq. (105) in Eq. (106) and then using Eq. (106) in Eq. (30). The final outcome is exactly Eq. (100), thus demonstrating that the formalism developed in this paper reduces to the correct low-intensity, first-order limit.

C. Results with radiation of wavelength 10.6 μm

Explicit numerical results are now exhibited for the case of a negative hydrogen ion irradiated by a monochromatic field of wavelength 10.6 μm . The binding energy of H^- is taken to be 0.75 eV. An intensity parameter of $z=1$ certainly can be considered an intense field, but this corresponds to only $1.1 \times 10^{10} \text{ W/cm}^2$ of 10.6- μm radiation, which is an intensity readily achieved with a large CO_2 laser. The transition probabilities which emerge from the calculation are such that intensity parameters up to $z=2$ or $z=3$ fall within the depletion limit set in Eq. (48), and discussed further in Sec. VI. In general, when explicit intensity effects are described, the value $z=1$ is selected as an example. However, in a few cases, the results are extended up to the intensity $z=10$, beyond the depletion limit accepted here, in order to illustrate in an exaggerated way some of the effects of intensity.

For the set of circumstances just prescribed, with $\lambda = 10.6 \mu\text{m}$ (or $\omega = 0.117 \text{ eV}$ in energy units) and $E_B = 0.75 \text{ eV}$ (or $\epsilon_B = 6.41$), the differential transition probability for circular polarization and for $z=1$ is shown in Fig. 2. This is the outcome of Eq. (98), in which the value of n_0 for $z=1$ is $n_0=8$. The shape of the angular distribution is quite smooth, rising to a prominent peak in the sideward direction. The forward direction in the circular polarization case is taken to be the direction of propagation of the field. The general character of the angular distribution remains much the same for all intensities, with lower intensities associated with a lower and broader peak, and higher intensities leading to a higher and narrower peak.

The angular distribution for linear polarization of the field exhibits much more structure and variability than does the circular polarization case. Figure 3 shows the results of Eq. (99) applied to a "low-intensity" case, where $z=10^{-3}$. (This corresponds to about 10^7 W/cm^2 of CO_2 laser radiation, which is not everyone's notion of low intensity.) The threshold order is $n_0=7$, and essentially the entire differential transition probability arises from this first term in the n sum. A double-peak structure is shown, with

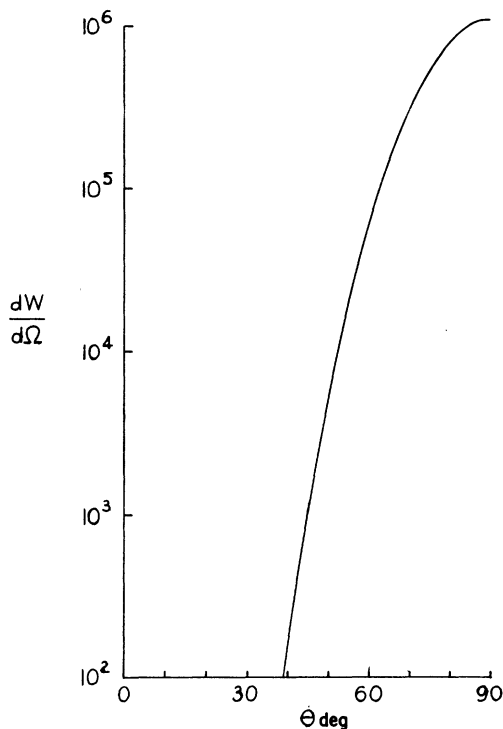


FIG. 2. Angular distribution of electrons photodetached from H^- by an intense circularly polarized plane wave of $10.6\text{-}\mu\text{m}$ wavelength. The intensity parameter is $z=1$. The forward direction is the direction of propagation of the field.

the peak in the forward direction being the larger of the two. For linear polarization, the forward direction is the direction of polarization of the field. An important general property of linear polarization is that the angular distributions for odd values of n share one set of characteristics, and even- n angular distributions exhibit a different set. Figure 3 is typical of odd- n behavior, with a maximum in the forward direction, and a zero at 90° . The zero in the sideward direction follows from the fact that α , given in Eq. (46), is zero at 90° , and from Eq. (B6), $J_n(z^{1/2}\alpha, -\frac{1}{2}z)$ vanishes when α does.

The differences between odd- n and even- n angular distributions are shown clearly in Fig. 4, which is a graph of Eq. (99) for $z=1$. In this case, the lowest order is $n_0=8$, but $n=9$ is also of major significance. Both $n=8$ and $n=9$ contributions are shown in Fig. 4, along with a total angular distribution arising from all orders. The distribution for $n=9$ shows the same maximum in the forward direction and zero in the sideward direction that was seen in Fig. 3, although there are now three peaks. The $n=8$ distribution, however, is quite small (although not zero) in the forward direction, has its first peak at about 45° , and

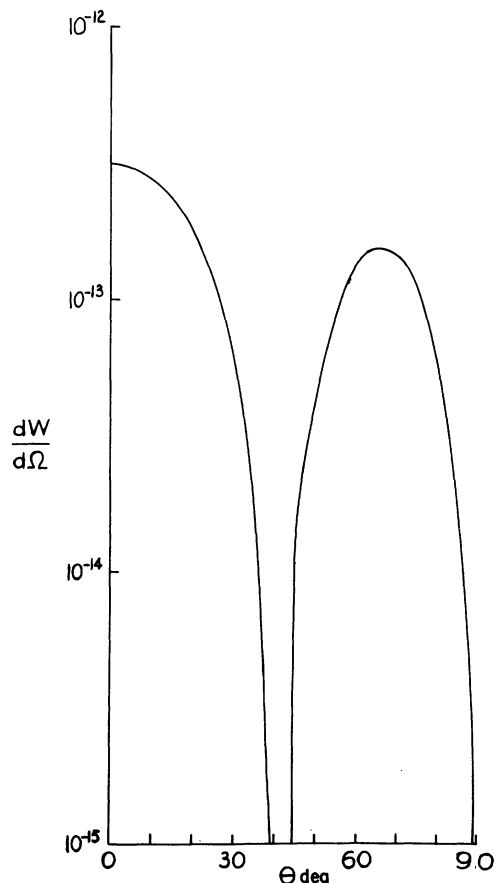


FIG. 3. Angular distribution of electrons photodetached from H^- by a low-intensity linearly polarized plane wave of $10.6\text{-}\mu\text{m}$ wavelength. The intensity parameter is $z=10^{-3}$. The forward direction is the polarization direction of the field.

shows a secondary peak in the sideward direction. The fact that $J_n(z^{1/2}\alpha, -z/2)$ is not zero when $\alpha=0$ and n is even follows from Eq. (B6). The total angular distribution in Fig. 4 has a fairly complicated structure. The complexity of this structure increases rapidly when larger values of z are considered.

When the angular distribution is integrated over solid angle, and the resulting total transition probability per unit time is plotted as a function of intensity, z , the rich diversity of structure seen in the angular distributions is smoothed over, and the relatively featureless curves shown in Figs. 5 and 6 arise for the circular and linear polarization cases, respectively. In each figure, the solid curve is the plot of calculated W versus z , whereas the dashed curve shows an extrapolation of the low-intensity result with a constant slope of seven in these logarithmic graphs. That is, the low-intensity limit contains contributions only from

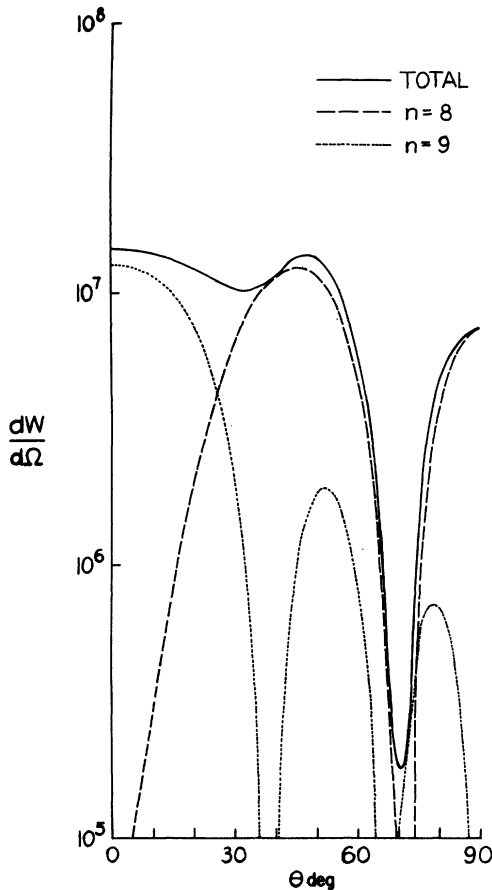


FIG. 4. Angular distribution of photons photodetached from H^- by an intense linearly polarized plane wave of $10.6\text{-}\mu\text{m}$ wavelength. The intensity parameter is $z=1$. The forward direction is the polarization direction of the field. The dashed curve is the contribution from the lowest order, $n_0=8$. The dotted curve is from $n=9$. The solid curve is the total contribution of all orders.

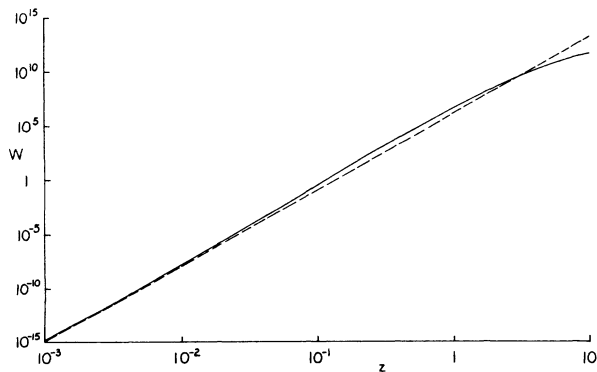


FIG. 5. Total transition probability per unit time for photodetachment of H^- by $10.6\text{-}\mu\text{m}$ circularly polarized radiation as a function of field intensity. The solid curve is the calculated result. The limit of reliability is at $z=3$. The dashed line is a constant-slope extrapolation of the low-intensity limit.

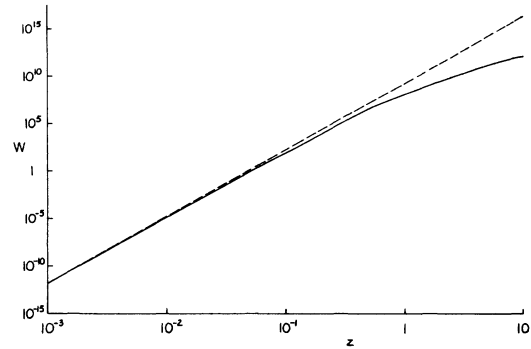


FIG. 6. Total transition probability per unit time for photodetachment of H^- by $10.6\text{-}\mu\text{m}$ linearly polarized radiation as a function of field intensity. The solid curve is the calculated result. The limit of reliability is at $z=3$. The dashed line is a constant-slope extrapolation of the low-intensity limit.

$n=7$, which is the value of n_0 when $z \rightarrow 0$, and thus $d(\log W)/d(\log z)=7$. The graphs are carried as far as $z=10$ in order to emphasize that the full calculated transition probability departs from straight-line behavior at high intensity. Nevertheless, up to $z=2$ or 3 , which is as far as the calculated results are trustworthy, the departure from linearity is not remarkable. These conclusions figure importantly in the discussion of possible demonstrations of the failure of perturbation theory, which will be given in Sec. IX.

The nearly featureless simplicity of Figs. 5 and 6 is largely an illusion. The total W -versus- z curves of Figs. 5 and 6 are repeated in Figs. 7 and 8, along with the separate contributions to W arising from n of 7, 8, and 9. In both circular and linear polarization cases, the lowest order, $n=7$, is the dominant contribution to the total transition probability when z is small. It then declines in importance, and finally falls to zero

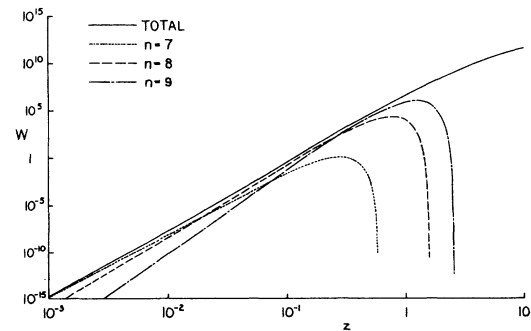


FIG. 7. Total transition probability per unit time for circular polarization as a function of intensity. The solid curve is the same as in Fig. 5, and represents the sum of all orders. The curves labeled $n=7$, 8 , and 9 give the separate contributions of those orders.

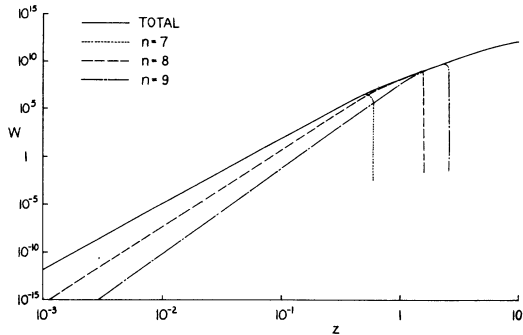


FIG. 8. Total transition probability per unit time for linear polarization as a function of intensity. The solid curve is the same as in Fig. 6, and represents the sum of all orders. The curves labeled $n=7$, 8 , and 9 give the separate contributions of those orders.

at $z=0.59$ since, according to Eq. (37), the lowest order which can contribute beyond $z=0.59$ is $n_0=8$. Recall that $\epsilon_B=6.41$ in this example. The eighth order contribution is dominant for a while, and goes to zero in its turn at $z=1.59$.

As z increases, not only does the order, n_0 , of the lowest-order contribution increase, but the relative contributions of terms with $n > n_0$ also increase. This can be seen to some degree in Figs. 7 and 8, but it is shown much more clearly in Figs. 9, 10, and 11. Figure 9 refers to circular polarization with $z=1$. It shows the partial contribution, W_n , of each order to the total transition probability per unit time, W . Not only does Fig. 9 show the most important order to be $n=10$, rather than the lowest order, $n_0=8$, but orders 9 through 14 are all important, and all give larger contributions than n_0 . This is an outcome quite startling from a perturbation-theory standpoint. In fact the intensity corresponding to $z=1$ lies beyond the radius of convergence of perturbation theory for this problem, as is shown in Sec. IX. For larger values of z , the pattern of W versus n broadens even more, with more different orders making important contributions, and with the peak value of n even farther removed from n_0 .

Figure 10 gives the variation of W_n with n for linear polarization with $z=1$. In this case, the lowest order does dominate, although the few following orders are significant. Actually, the lowest order remains dominant in the linear polarization case even when z is larger than unity. The effect of increasing intensity is to enlarge the set of orders which make an important contribution to the total W . This is shown in exaggerated form in Fig. 11, for the unacceptably [for Eq. (99)] large value $z=10$. The lowest order here is $n_0=17$. Orders as large as $n=30$ remain significant.

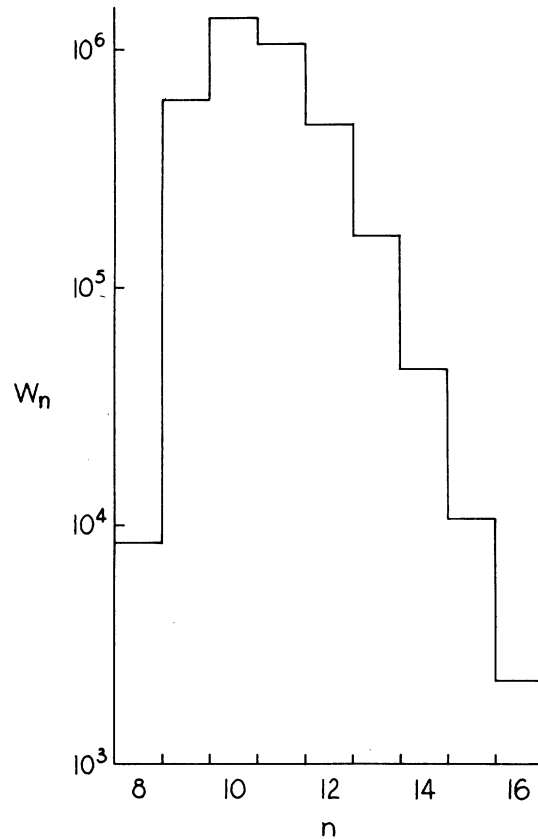


FIG. 9. The partial contribution, W_n , of each order n to the total transition probability per unit time for photo-detachment of H^- by circularly polarized $10.6\text{-}\mu\text{m}$ radiation at $z=1$. The lowest order is $n_0=8$.

D. Comparison of circular and linear polarization results

In Sec. IV, the ratio of transition probability arising from circular polarization to that associated with linear polarization was evaluated for arbitrary ϵ_B in the low intensity, or perturbation limit. The circular-to-linear ratio thus found, has the value 1.04×10^{-3} for $\epsilon_B=6.41$, appropriate to the H^- ion in $10.6\text{-}\mu\text{m}$ radiation. This result comes directly from Eq. (62).

A more novel type of polarization comparison will now be made. With ϵ_B set at the value for H^- in $10.6\text{-}\mu\text{m}$ radiation, the effect of intensity on the circular-to-linear ratio is explored. The results are shown in Fig. 12. The ratio shows a striking rise as the intensity increases. When $z=10^{-3}$, the ratio has essentially the zero-intensity limiting value of 10^{-3} . This increases to about 4×10^{-2} at $z=1$, and rises further to about 10^{-1} when z is in the neighborhood of 2 or 3, which is about the limit of validity of the calculations. The rate of increase of the circular-to-linear ratio has begun to diminish at this inten-

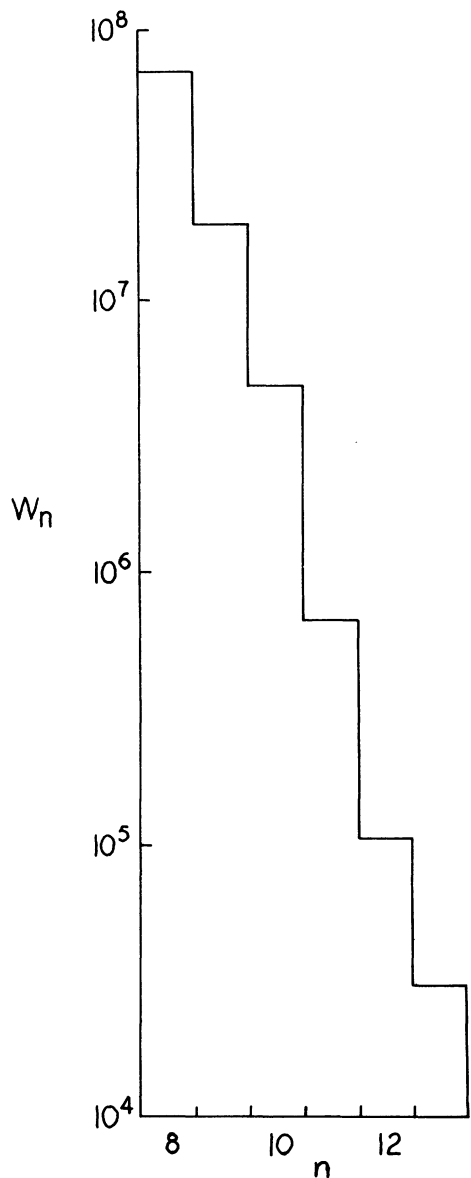


FIG. 10. The partial contribution, W_n , of each order n to the total transition probability per unit time for photodetachment of H^- by linearly polarized $10.6\text{-}\mu\text{m}$ radiation at $z=1$. The lowest order is $n_0=8$.

sity, and this trend toward leveling off is shown by plotting the ratio as far as $z=10$.

The spectacular hundredfold increase in the circular-to-linear ratio between the small-intensity limit and the region around $z=3$ is probably the most striking of all specific intensity effects. Its physical basis is easily understood. The reason linear polarization dominates circular polarization for high-order processes in the low-intensity limit is that there are many more angular momentum substates available in the linear case. The

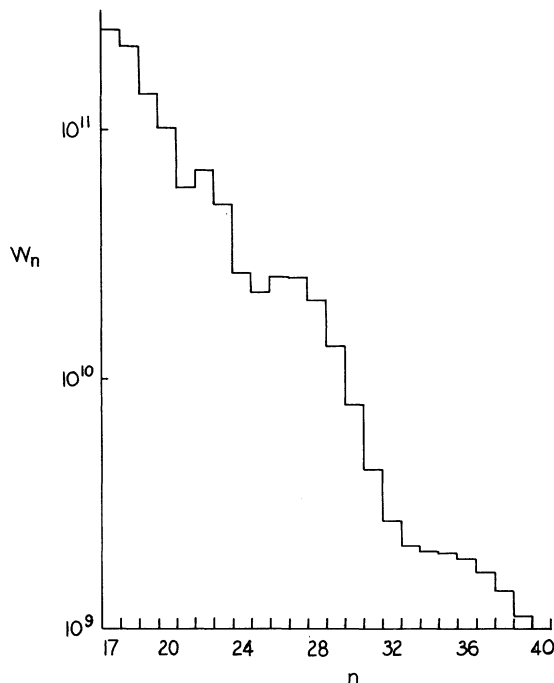


FIG. 11. The partial contribution, W_n , of each order n to the total transition probability per unit time for photodetachment of H^- by linearly polarized $10.6\text{-}\mu\text{m}$ radiation at $z=10$. The lowest order is $n_0=17$. The intensity is too high for the results to be reliable. The intent of this figure is to show the nature of the change from Fig. 10.

ground state of H^- is an S state, and an interaction with the field of order n_0 leads to a final state which can have only the angular momentum $l=n_0$ for circularly polarized radiation, but can have any of alternate angular momentum states between

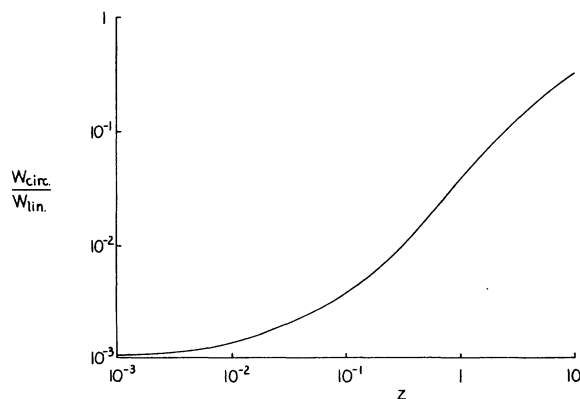


FIG. 12. Transition probability for photodetachment of H^- by $10.6\text{-}\mu\text{m}$ radiation by a circularly polarized field as compared to a linearly polarized field. The ratio is plotted as a function of field intensity, z . The limit of reliability is $z=3$.

$l=0$ and $l=n_0$ for the linearly polarized case. That is, the comparison is between a single channel in the circular case, and either $\frac{1}{2}n_0 + 1$ (for n_0 even) or $\frac{1}{2}(n_0 + 1)$ (for n_0 odd) channels in the linear case.¹⁰ However, when the intensity increases, processes with $n > n_0$ become increasingly important. A comparison of Figs. 9 and 10 shows that both the number of higher-order states which contribute, and the relative importance of each of these higher-order states, are much larger for circular than for linear polarization. In the circular case, therefore, the extra channels which open up due to the $n > n_0$ states as z increases are more important than for the linear case. There is thus a tendency for circular polarization to regain some of its importance relative to linear polarization when z increases, even though n_0 is large.

VIII. APPLICATION TO H

Photoionization of the initially neutral hydrogen atom is not a problem which really suits the validity conditions given in Secs. II and III D because of the possibility of bound-state resonances, and because of the long range of the Coulomb interaction between the detached electron and the residual positive ion. Nevertheless, the present theory might have some relevance to the hydrogen atom problem, and some interesting results can be shown.

The basic expressions stated in Eqs. (32) and (45) require for their application only a knowledge of the appropriate momentum-space wave function, $\hat{\phi}_i(\vec{p})$. If the hydrogen atom is initially in its ground state, with the configuration-space wave function

$$\phi_i(\vec{r}) = (\pi a_0^3)^{-1/2} \exp(-r/a_0),$$

where a_0 is the Bohr radius, then

$$\hat{\phi}_i(\vec{p}) = \frac{2^3(\pi a_0^3)^{1/2}}{(1+p^2 a_0^2)^2} \quad (107)$$

from Eq. (13). General results can now be calculated from Eqs. (32) and (45).

Only the low-intensity, first-order result will be considered here. From Eqs. (58) and (107), this is

$$\frac{dW}{d\Omega} = \frac{2^5}{\pi} a_0^3 (2m^3 \omega^5)^{1/2} (1 - \epsilon_B)^{3/2} \frac{z \cos^2 \theta}{(1 + p^2 a_0^2)^4}. \quad (108)$$

When divided by the incoming flux, given in Eq. (59), the expression (108) becomes the differential cross section

$$\frac{d\sigma}{d\Omega} = \frac{2^5 \alpha_0 (p a_0)^3}{m \omega} \frac{\cos^2 \theta}{(1 + p^2 a_0^2)^4}, \quad (109)$$

after using the kinematical relationship

$$(1 - \epsilon_B) = p^2 / 2m\omega,$$

which arises from Eq. (33) in the low-intensity first-order limit. Equation (109) corresponds to the standard textbook result²⁷ for the photoelectric effect in hydrogen when the final state is approximated as a plane wave. The applied field is treated in dipole approximation in arriving at Eq. (109).

Another instructive remark that can be made about hydrogen concerns the intensity parameter, z_1 . This parameter is defined in Eq. (74). For hydrogen,

$$2mE_B = a_0^{-2},$$

where a_0 is the Bohr radius, and thus z_1 is

$$z_1 = e^2 a^2 a_0^2, \quad (110)$$

exactly of the form of Eq. (84). As discussed in Sec. V C, z_1 is explicitly a bound-state intensity parameter, and should be expected to be more important in the hydrogen atom problem than is z . The parameter z is more important than z_1 in the negative ion problem. The form of z_1 shown in Eq. (110) has previously been identified^{28,29} as the relevant intensity parameter for electromagnetic interactions with hydrogen atoms.

IX. CONVERGENCE OF PERTURBATION THEORY

In this section, the radius of convergence of a perturbation expansion will be found for one of the closed forms achieved above for a transition probability expression. This sets the stage for references about perturbation expansions in other problems in electrodynamics. In particular, it may have bearing on an experimental investigation of intense-field behavior.⁹

When an expression such as Eq. (98) or Eq. (99) is expanded in powers of z , the power series so formed is a perturbation expansion of the differential transition probability. The reason is that the intensity parameter, z , as defined in Eq. (17) can also be written as

$$z = \alpha_0 \rho \lambda^2 \lambda_c. \quad (111)$$

Thus, an expansion in powers of z is equivalent to an expansion in powers of α_0 , the fine-structure constant. In Eq. (111), λ_c is the Compton wavelength of the electron, λ is the wavelength of the applied field (where $\lambda \equiv \lambda/2\pi$), and ρ is the energy density of the field divided by ω . In other words, ρ can be viewed as the "photon" density of the field, since it is the field energy density divided by the energy of a single photon of energy $\hbar\omega$. The physical significance of the intensity parameter, z , is evident from Eq. (111). It is

just the product of the fundamental electromagnetic field-charged particle coupling strength α_0 , times the number of "photons" contained in an effective interaction volume $\chi^2 \lambda_c$. It really should be expected that the interaction between the electromagnetic field and a charged particle should involve more than just the basic coupling constant, α_0 . The electromagnetic field is a boson field, and the more particles there are in a given mode, the stronger the interaction should be. The significance of this "gregarious" nature of bosons in an intense-field problem has been remarked upon previously.³⁰

It is not possible to do a general exploration of the perturbation expansion properties of Eqs. (32) and (45), because $|\hat{\phi}_i(\vec{p})|^2$ is unspecified in these equations, and p is a function of z as a result of the conservation condition, Eq. (33). This shortcoming does not apply to the specific results for H^- stated in Eqs. (98) and (99). The complexities of the generalized Bessel function make the analytical properties of Eq. (99) quite difficult to explore,¹¹ and so attention will be focused on Eq. (98).

The radius of convergence of an expansion of Eq. (98) as a function of z is quite easy to establish. The argument of the Bessel function is $z^{1/2}\gamma$, with γ a function of z as shown in the definition Eq. (34). Since the Bessel function can be written as

$$J_n(z^{1/2}\gamma) = \left(\frac{1}{2}z^{1/2}\gamma\right)^n \sum_{k=0}^{\infty} f_k(z\gamma^2), \quad (112)$$

then the squared Bessel function is

$$J_n^2(z^{1/2}\gamma) = \left(\frac{1}{4}z\gamma^2\right)^n \sum_{k=0}^{\infty} f_k(z\gamma^2) \sum_{l=0}^{\infty} f_l(z\gamma^2). \quad (113)$$

Since $J_n(\xi)$ is an analytic function of ξ for all complex ξ such that $|\xi| < \infty$, then $\sum f_k(\xi)$ as it appears in Eq. (112) is also an entire function of ξ . Then from Eq. (113), $J_n^2(z^{1/2}\gamma)$ is an entire function of $z\gamma^2$. The only singularities in Eq. (98) thus arise from the branch point in each term in the series at $z = n - \epsilon_B$ contributed by the $(n - z - \epsilon_B)^{1/2}$ factors. The radius of convergence of an expansion in z is given by the singularity nearest to the origin. That is, this radius of convergence is

$$z < n_0 - \epsilon_B = [\epsilon_B] - \epsilon_B, \quad (114)$$

from Eq. (37). The square bracket in Eq. (114) signifies the smallest integer containing the quantity within the bracket. The radius of convergence given by Eq. (114) is illustrated in Fig. 13 as a function of ϵ_B . For example, in the problem of H^- photodetachment by 10.6- μm radiation, $\epsilon_B = 6.41$, $[\epsilon_B] = 7$, and so Eq. (114) gives $z < 0.59$.

In the light of Eq. (37), it is clear by inspection

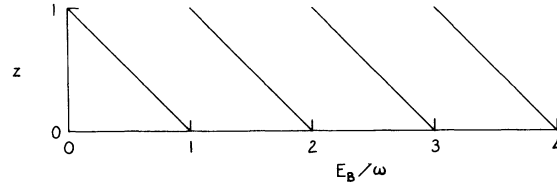


FIG. 13. The radius of convergence of a perturbation expansion of Eq. (98), the differential transition probability for photodetachment of H^- by circularly polarized radiation. The radius of convergence is plotted against E_B/ω , the binding energy expressed in units of a photon energy.

that the radius of convergence of Eq. (98) cannot exceed the limit stated in Eq. (114). Should z exceed the value in (114), the value of n_0 is indexed upward by one unit according to Eq. (37), and this sudden dropping of a term from the sum over n is nonanalytic behavior.

It is instructive to examine the numerical results developed from Eq. (98) to see the nature of the effects manifested when the perturbation limit is exceeded. The angular distribution in Fig. 2 shows nothing unusual. This figure is for $z = 1$, which is beyond the radius of convergence, but smaller z values yield angular distributions much the same as Fig. 2, only lower and broader. Figure 5 also shows nothing unusual in the neighborhood of $z = 0.59$. The curve remains quite smooth, nearly straight, and quite close to the low-intensity slope. The resolution of the graph of Fig. 5 into its components, as in Fig. 7, gives the first indication of failure of perturbation theory. The low-intensity lowest order, $n_0 = 7$, ceases to contribute at $z = 0.59$, and higher-order terms take over. This is not evident in the total transition probability, but it is manifested in the polarization ratio results of Fig. 12, where, as discussed in Sec. VII D, the significant contributions of higher-order terms ease the angular momentum constraints associated with circular polarization. Other evidence of the failure of perturbation theory is clearly to be seen in Fig. 9, where the most important order is two orders higher than the lowest order, and even the fifteenth-order term is more important than the eighth (lowest) order. Experimental detection of this phenomenon would require energy resolution of the photodetached electrons, in order to determine the order of the process causing detachment, as established by Eq. (35).

The next step is to inquire about the relationship of Eq. (98) to the exact analytical expression for the photoionization of H^- by a circularly polarized plane wave. Equation (98) falls short in two respects. One limitation is that the ground-state

wave function employed for H^- is not exact, but is simply an analytical approximation.⁸ In view of the lack of a precise analytical form for this wave function, there is no remedy for this defect. However, a very large class of possible $\hat{\phi}_i(\vec{p})$ functions will give rise to the result (114), in view of the fact that the limiting singularity was not contributed by $|\hat{\phi}_i(\vec{p})|^2$, but was preexisting in Eq. (32). It is thus not unreasonable to conjecture that Eq. (114) is a generally valid outcome of Eq. (98). If it is supposed that Eq. (98) really is an exact application of Eq. (32) to the H^- problem, what then, are the limitations of Eq. (32)? The most fundamental limitation is the approximate nature of Eq. (3), which is at the heart of all subsequent results. No further analysis is possible without a formal expression for correction terms to Eq. (3). None is available, but it is instructive nevertheless to consult Eq. (A18), which would be a complete formal expression for the S matrix were V_B not influenced by the applied field. Equation (32) represents the contribution of the first term in Eq. (A18). The second term has been neglected. However, the structure of the inner products in the second term in (A18) is such that one always contains a V_A interaction term, and the other contains V_B . The leading term in Eq. (A18) contains no V_B at all, except indirectly in ψ_B (which is also in the second term). Thus, the presence of the V_B operator in the second term gives it an analytical structure distinct from the first term. New singularities in the z plane can be introduced by the second term, but the branch points from the first term cannot be canceled by the second term. Therefore, the radius of convergence in Eq. (114) can be reduced, but not enlarged, if it were possible to consider the complete analytical structure of the full transition probability. Equation (114) is an upper bound (though not necessarily a least upper bound) for the radius of convergence.

Some inferences for other physical problems can be drawn from the H^- results analyzed here. Lompre, *et al.*⁹ have conducted high-order multiphoton ionization experiments on noble gases at very high field intensity, and find no departure from $d(\log W)/d(\log z_1) = n_0$, where n_0 is the low-intensity limiting slope. The relevant intensity parameter for this atomic photoionization problem should be essentially the z_1 of Eq. (74), (84), or (110). As stated earlier, this is related to the Keldysh intensity parameter γ by $z_1 = \gamma^{-2}$. Lompre, *et al.* carry their experiments with 1.06- μm radiation as far as 10^{15} W/cm², where $z_1 \approx 10$. Since this appears to be a true intense-field environment, they note with great interest the maintenance of a constant slope in the logarithmic

graph of transition probability versus intensity. This may very well be a phenomenon of the same sort indicated in Fig. 5, where a nearly constant value of $d(\log W)/d(\log z)$ is maintained well beyond the failure point of perturbation theory. The difficulty is that total-yield experiments simply do not offer a sensitive test of the failure of perturbative behavior (or the onset of explicit intense-field behavior).

APPENDIX A: S-MATRIX FORMALISM WITH TWO POTENTIALS

The usual S -matrix formalism for transitions induced in a system will be extended here to the case where there are two distinct independent interaction terms. Initially, both interactions will be considered to be of equivalent importance, and both can be time dependent. Distinctions between the interaction terms will be introduced as the formalism is developed.

The system under consideration is described in full by the equation in the Schrödinger picture

$$(i\partial_t - H_0 - V_A - V_B)\Psi = 0, \quad (\text{A1})$$

where V_A and V_B can both be time dependent; H_0 , V_A , V_B are Hilbert space operators, Ψ is a vector in Hilbert space, t is a parameter external to the Hilbert space, and $i\partial_t$ is implicitly multiplied by the unit operator of the Hilbert space. It is presumed that the solution vectors Ψ_A , Ψ_B to the equations

$$(i\partial_t - H_0 - V_A)\Psi_A = 0, \quad (\text{A2})$$

$$(i\partial_t - H_0 - V_B)\Psi_B = 0, \quad (\text{A3})$$

are known. The corresponding Green's operators satisfy the equations

$$(i\partial_t - H_0 - V_A)G_A(t, t_0) = \delta(t - t_0), \quad (\text{A4})$$

$$(i\partial_t - H_0 - V_B)G_B(t, t_0) = \delta(t - t_0), \quad (\text{A5})$$

with a unit operator of the Hilbert space implicit on the right-hand side. The retarded solution of Eq. (A4) is

$$G_A^{(+)}(t, t_0) = -i\Theta(t - t_0) \sum_j |A, j, t\rangle \langle A, j, t_0|, \quad (\text{A6})$$

where, for convenience, Dirac bra-ket notation is used for the state vectors with the correspondence

$$\Psi_{Aj}(t) \leftrightarrow |A, j, t\rangle,$$

and the index j represents all the quantum numbers which define the state. The advanced solution of Eq. (A4) is

$$\begin{aligned} G_A^{(-)}(t, t_0) &= G_A^{(+)*}(t_0, t) \\ &= i\Theta(t_0 - t) \sum_j |A, j, t\rangle \langle A, j, t_0|. \end{aligned} \quad (\text{A7})$$

The retarded and advanced Green's operator solutions of Eq. (A5) are, of course, of the same form as Eqs. (A6) and (A7). The action of the Green's operator on a state vector is seen immediately to be

$$G_A^{(+)}(t, t_0)\Psi_A(t_0) = -i\Theta(t - t_0)\Psi_A(t), \quad (\text{A8})$$

$$G_A^{(-)}(t, t_0)\Psi_A(t_0) = i\Theta(t_0 - t)\Psi_A(t). \quad (\text{A9})$$

The solution of Eq. (A1) is expressible either as

$$\Psi^{(+)}(t) = \Psi_A(t) + \int dt_1 G_A^{(+)}(t, t_1) V_B(t_1) \Psi^{(+)}(t_1), \quad (\text{A10})$$

or as

$$\Psi^{(+)}(t) = \Psi_B(t) + \int dt_1 G_B^{(+)}(t, t_1) V_A(t_1) \Psi^{(+)}(t_1). \quad (\text{A11})$$

Up to this point, the interaction operators V_A and V_B have been treated entirely symmetrically. Now it will be supposed that V_A is turned off at asymptotic times, but V_B is not; and it is the transitions caused by V_A which are to be calculated.

The transition S matrix may then be expressed either in terms of the in-state $\Psi^{(+)}$ as

$$S_{fi} = \lim_{t \rightarrow \infty} (\Psi_{Bf}, \Psi_i^{(+)}), \quad (\text{A12})$$

or in terms of the out-state $\Psi^{(-)}$ as

$$S_{fi} = \lim_{t \rightarrow -\infty} (\Psi_f^{(-)}, \Psi_{Bi}), \quad (\text{A13})$$

where the subscripts i and f represent initial and final conditions, respectively. The physical meaning of Eq. (A12), for example, is that the S matrix is the probability amplitude that an in-state of the complete system (including both V_A and V_B) will, at infinite time, be in some particular state of the system in which only V_B is present.

The form of the S matrix in Eq. (A12) will be examined first. For $\Psi_i^{(+)}$, the solution given in Eq. (A11) will be used, since this result contains Ψ_B as the homogeneous term. Direct substitution gives

$$\begin{aligned} S_{fi} &= \lim_{t \rightarrow \infty} (\Psi_{Bf}, \Psi_{Bi}) + \lim_{t \rightarrow \infty} \int dt_1 (\Psi_{Bf}(t), G_B^{(+)}(t, t_1) V_A(t_1) \Psi_i^{(+)}(t_1)) \\ &= \delta_{fi} + \lim_{t \rightarrow \infty} \int dt_1 (G_B^{(+)}(t_1, t) \Psi_{Bf}(t), V_A(t_1) \Psi_i^{(+)}(t_1)). \end{aligned}$$

If Eq. (A9) is used with subscript B , then the only appearance of time t in the integrand is in the theta function. The infinite-time limit is

$$\lim_{t \rightarrow \infty} \Theta(t - t_1) = 1,$$

so the S matrix takes the form

$$S_{fi} = \delta_{fi} - i \int dt_1 (\Psi_{Bf}, V_A \Psi_i^{(+)})_{t_1}, \quad (\text{A14})$$

where the subscript t_1 on the scalar product in the integrand means that all factors in that product have the argument t_1 . By repeated use of Eqs. (A11) or (A10), the expression in (A14) can be expanded in powers of V_A or V_B . Suppose Eq. (A11) is used in (A14), and δ_{fi} is included with S_{fi} . This gives

$$\begin{aligned} (S - 1)_{fi} &= -i \int dt_1 (\Psi_{Bf}, V_A \Psi_{Bi})_{t_1} \\ &\quad - i \int dt_1 \int dt_2 (\Psi_{Bf}(t_1), V_A(t_1) G_B^{(+)}(t_1, t_2) V_A(t_2) \Psi_i^{(+)}(t_2)), \end{aligned} \quad (\text{A15})$$

which can be further expanded by repeated use of Eq. (A11). Equation (A15) is a conventional perturbation expression in which V_B could have been incorporated in H_0 , and V_A treated as the only perturbing potential. Of more interest here is the case in which an expansion in powers of V_B is more tractable than an expansion in powers of V_A . An expansion in powers of V_B is commenced by the substitution of Eq. (A10) in Eq. (A14). The result is then

$$\begin{aligned} (S - 1)_{fi} &= -i \int dt_1 (\Psi_{Bf}, V_A \Psi_{Ai})_{t_1} \\ &\quad - i \int dt_1 \int dt_2 (\Psi_{Bf}(t_1), V_A(t_1) G_A^{(+)}(t_1, t_2) V_B(t_2) \Psi_i^{(+)}(t_2)). \end{aligned} \quad (\text{A16})$$

Repeated substitution of Eq. (A10) in Eq. (A16) gives a series in which V_A appears once in each term, and V_B appears with successively higher powers in each term.

If Eq. (A13) is used in place of (A12) as the defining expression for the S matrix, then the result corresponding to Eq. (A16) is

$$(S-1)_{fi} = -i \int dt_1 (\Psi_{A_f}, V_A \Psi_{B_i})_{t_1} - i \int dt_1 \int dt_2 (\Psi_f^{(-)}(t_2), V_B(t_2) G_A^{(+)}(t_2, t_1) V_A(t_1) \Psi_{B_i}(t_1)). \quad (\text{A17})$$

As in Eq. (A16), repeated substitution of Eq. (A10) in Eq. (A17) gives a perturbation expansion in V_B . A useful form of Eq. (A17) is obtained by replacing the Green's operator with expression (A6) to yield

$$(S-1)_{fi} = -i \int dt_1 (\Psi_{A_f}, V_A \Psi_{B_i})_{t_1} + (-i)^2 \sum_j \int dt_1 \int dt_2 \Theta(t_2 - t_1) (\Psi_f^{(-)}, V_B \Psi_{A_j})_{t_2} (\Psi_{A_j}, V_A \Psi_{B_i})_{t_1}. \quad (\text{A18})$$

APPENDIX B: GENERAL PROPERTIES OF THE GENERALIZED BESSEL FUNCTION $J_n(u, v)$

A generalized Bessel function of integer order may be defined by

$$J_n(u, v) = (2\pi)^{-1} \int_{-\pi}^{\pi} d\theta \exp[i(u \sin\theta + v \sin 2\theta - n\theta)]. \quad (\text{B1})$$

The infinite series representation

$$J_n(u, v) = \sum_{k=-\infty}^{\infty} J_{n-2k}(u) J_k(v) \quad (\text{B2})$$

can be derived from Eq. (B1), or can be used as the defining relation. The series representation can be used to extend the definition to arbitrary orders if desired. Functions closely related to $J_n(u, v)$ have been identified and explored to some degree since the early work^{11,31-34} on linearly polarized intense fields, but not in a systematic way.

For purposes of numerical calculation, the doubly infinite sum of Eq. (B2) is more conveniently cast in the form

$$J_n(u, v) = J_0(u) J_{n/2}(v) + \sum_{k=1}^{\infty} J_{2k}(u) [J_{k+n/2}(v) + J_{k-n/2}(v)] \quad (\text{B3})$$

for even n , or in the form

$$J_n(u, v) = \sum_{k=1}^{\infty} J_{2k-1}(u) [J_{k+(n-1)/2}(v) - J_{k-(n-1)/2}(v)] \quad (\text{B4})$$

for odd n .

From either Eq. (B1) or (B2) it follows immediately that

$$J_n(u, 0) = J_n(u) \quad (\text{B5})$$

and

$$J_n(0, v) = \begin{cases} J_{n/2}(v), & n \text{ even} \\ 0, & n \text{ odd.} \end{cases} \quad (\text{B6})$$

Further direct results are

$$\begin{aligned} J_n(-u, v) &= (-)^n J_n(u, v), \\ J_n(u, -v) &= (-)^n J_{-n}(u, v). \end{aligned} \quad (\text{B7})$$

The standard recurrence relations for the Bessel functions have their analogs with the $J_n(u, v)$. It follows directly from Eq. (B1) or (B2) that

$$J_{n-1}(u, v) - J_{n+1}(u, v) = 2\partial_u J_n(u, v) \quad (\text{B8})$$

and

$$J_{n-2}(u, v) - J_{n+2}(u, v) = 2\partial_v J_n(u, v). \quad (\text{B9})$$

An integration by parts in Eq. (B1) yields

$$\begin{aligned} 2nJ_n(u, v) &= u[J_{n-1}(u, v) + J_{n+1}(u, v)] \\ &\quad + 2v[J_{n-2}(u, v) + J_{n+2}(u, v)]. \end{aligned} \quad (\text{B10})$$

Various other results can be obtained by combinations of Eqs. (B8)–(B10), for example,

$$\begin{aligned} u\partial_u J_n(u, v) + 2v\partial_v J_n(u, v) &= nJ_n(u, v) - uJ_{n+1}(u, v) \\ &\quad - 2vJ_{n+2}(u, v), \end{aligned}$$

$$\begin{aligned} u\partial_u J_n(u, v) + 2v\partial_v J_n(u, v) &= -nJ_n(u, v) + uJ_{n-1}(u, v) \\ &\quad + 2vJ_{n-2}(u, v), \end{aligned}$$

$$\frac{1}{2}\partial_v J_n(u, v) = \partial_u J_{n-1}(u, v) + \partial_u J_{n+1}(u, v).$$

Two important theorems can be proved from Eq. (B1). One is that

$$\sum_{n=-\infty}^{\infty} e^{in\phi} J_n(u, v) = \exp[i(u \sin\phi + v \sin 2\phi)], \quad (\text{B11})$$

which corresponds directly to the generating function relation for the Bessel functions. The other theorem is

$$\sum_{k=-\infty}^{\infty} J_{n+k}(u, v) J_k(u', v') = J_n(u \pm u', v \pm v'), \quad (\text{B12})$$

which is analogous to Neumann's addition theorem for the Bessel functions, and which has various useful special cases.

Small-argument results for $J_n(u, v)$ are easily

stated if only one argument is small. For $|v| \ll 1$, the first-order result is

$$J_n(u, v) \approx J_n(u) + \frac{1}{2}v[J_{n-2}(u) - J_{n+2}(u)], \quad (\text{B13})$$

with various other forms available through use of the recurrence relations. When $|u| \ll 1$ and n is odd, one has

$$J_n(u, v) \approx \frac{1}{2}u[J_{(n-1)/2}(v) - J_{(n+1)/2}(v)]. \quad (\text{B14})$$

When $|u| \ll 1$ and n is even the lowest order in u is quadratic, and is

$$J_n(u, v) \approx \left[1 - \frac{u^2}{4} \left(1 - \frac{n}{2v}\right)\right] J_{n/2}(v). \quad (\text{B15})$$

The case when both arguments are small, and $|v| = 0(|u|^2)$ is treated in Appendix C.

Asymptotic results for $J_n(u, v)$ depend upon the relative magnitudes of n , u , and v , and generally involve complicated expressions. Asymptotic results for the case of direct interest here are given in Appendix D. The partial differential equation satisfied by $J_n(u, v)$ is too complicated to be particularly interesting. The results given in

this appendix represent just a sampling of some of the more easily proved properties of the $J_n(u, v)$ functions.

APPENDIX C: SMALL-ARGUMENT LIMIT OF THE GENERALIZED BESSEL FUNCTION $J_n(u, v)$

The particular limit to be found is

$$\lim_{z \rightarrow 0} J_n(z^{1/2} \mu, zv),$$

where z is a positive real number. That is, the notation is introduced that

$$u = z^{1/2} \mu, \quad v = zv, \quad (\text{C1})$$

and z is here a small parameter.

For even n , the form (B3) can be used. The lowest order in which z appears in $J_0(u)J_{n/2}(v)$ is $n/2$. The product $J_{2k}(u)J_{k+n/2}(v)$ contributes terms of minimum order $2k + n/2$ in z , and since the k sum starts at $k=1$, this term can be neglected. The product $J_{2k}(u)J_{-k+n/2}(v)$ contributes terms of minimum order $n/2$ in z for $k \leq n/2$. The function $J_n(z^{1/2} \mu, zv)$ thus behaves as $z^{n/2}$ for small z , and is given by

$$\begin{aligned} \lim_{z \rightarrow 0} J_n(z^{1/2} \mu, zv) &= \lim_{z \rightarrow 0} \left(J_0(z^{1/2} \mu) J_{n/2}(zv) + \sum_{k=1}^{n/2} J_{2k}(z^{1/2} \mu) J_{-k+n/2}(zv) \right) \\ &= \lim_{z \rightarrow 0} \left[\frac{1}{(\frac{1}{2}n)!} \left(\frac{zv}{2}\right)^{n/2} + \sum_{k=1}^{n/2} \frac{1}{(2k)!} \left(\frac{z^{1/2} \mu}{2}\right)^{2k} \frac{1}{(-k + \frac{1}{2}n)!} \left(\frac{zv}{2}\right)^{-k+n/2} \right] \\ &= \lim_{z \rightarrow 0} \left(\frac{zv}{2}\right)^{n/2} \sum_{k=0}^{n/2} \frac{(\mu^2/2v)^k}{(2k)! (\frac{1}{2}n - k)!}. \end{aligned} \quad (\text{C2})$$

The same type of analysis for odd values of n , starting from Eq. (B4), gives

$$\begin{aligned} \lim_{z \rightarrow 0} J_n(z^{1/2} \mu, zv) &= \lim_{z \rightarrow 0} \sum_{k=1}^{(n+1)/2} [J_{2k-1}(z^{1/2} \mu) J_{-k+(n+1)/2}(zv)] \\ &= \lim_{z \rightarrow 0} \left(\frac{zv}{2}\right)^{n/2} \sum_{k=0}^{(n-1)/2} \frac{(\mu^2/2v)^{k+1/2}}{(2k+1)! [\frac{1}{2}(n-1) - k]!}. \end{aligned} \quad (\text{C3})$$

In each case, the result contains a factor $z^{n/2}$, and a finite sum depending on μ , v , and n .

APPENDIX D: ASYMPTOTIC LIMIT OF THE GENERALIZED BESSEL FUNCTION $J_n(u, v)$

Many possible asymptotic limits exist for $J_n(u, v)$, depending on the relative magnitudes of the order and the two arguments. The case that will be investigated here is the most general case that is relevant to the physical problem presented in this paper. Specifically, the conditions of interest are

$$\begin{aligned} u &= z^{1/2} \alpha, \quad v = -z/2, \\ \alpha &= 8^{1/2} (n - z - \epsilon_B)^{1/2} \cos \theta, \\ n &\geq z + \epsilon_B, \\ n, z, \epsilon_B &, \text{ real and positive,} \\ z &\gg 1, \end{aligned} \quad (\text{D1})$$

where the u, v parameters are as they appear in Eq. (45), α is defined in Eq. (46), the lower limit of n is as shown in Eq. (36), and $\epsilon_B \equiv E_B/\omega$. The asymptotic nature of the problem is fixed by the large magnitude of the intensity parameter, z ,

which requires large magnitudes for n , u , v .

From Eq. (B1), the function to be explored can be written as

$$J_n(z^{1/2}\alpha, -z/2) = (2\pi)^{-1} \int_{-\pi}^{\pi} d\phi e^{zg(\phi)}, \quad (\text{D2})$$

where

$$\begin{aligned} g(\phi) &= i(\alpha z^{-1/2} \sin\phi - \frac{1}{2} \sin 2\phi - n\phi/z), \\ g'(\phi) &= i(\alpha z^{-1/2} \cos\phi - \cos 2\phi - n/z), \quad (\text{D3}) \\ g''(\phi) &= i(-\alpha z^{-1/2} \sin\phi + 2 \sin 2\phi). \end{aligned}$$

The saddle points of $g(\phi)$ in the complex ϕ plane are found from $g'(\phi) = 0$, which gives

$$\cos^2\phi_0 - \frac{\alpha}{2z^{1/2}} \cos\phi_0 + \frac{1}{2} \left(\frac{n}{z} - 1 \right) = 0, \quad (\text{D4})$$

where ϕ_0 designates the saddle point. The solutions of Eq. (D4) are

$$\cos\phi_0 = \frac{1}{4z^{1/2}} \{ \alpha \pm i [8(n-z) - \alpha^2]^{1/2} \}. \quad (\text{D5})$$

From the definition of α in Eq. (D1), the radicand in Eq. (D5) is

$$\begin{aligned} 8(n-z) - \alpha^2 &= 8[(n-z - \epsilon_B) \sin^2\phi + \epsilon_B] \\ &\geq 8\epsilon_B, \quad (\text{D6}) \end{aligned}$$

where the inequality follows from $n \geq z + \epsilon_B$ as given in Eq. (D1). The saddle points, therefore, are not on the real axis. This is made explicit by setting

$$\sin\phi_0 = \pm (2z^{1/2})^{-1} \{ (n+z - \frac{1}{4}\alpha^2 + [(n+z)^2 - z\alpha^2]^{1/2})^{1/2} - i \{ -n-z + \frac{1}{4}\alpha^2 + [(n+z)^2 - z\alpha^2]^{1/2} \}^{1/2} \}. \quad (\text{D10})$$

This, together with $\cos\phi_0$ in Eq. (D5), gives all the information necessary to fix $g(\phi_0)$ and $g''(\phi_0)$. At one saddle point, the upper sign is to be used in both Eqs. (D5) and (D10), and the lower sign in both (D5) and (D10) is associated with the second saddle point which lies along the deformed path of integration.

With $g(\phi_0)$, $g''(\phi_0)$ expressed by means of Eqs. (D5) and (D10), and the results employed in Eq. (D9), the asymptotic form thus found for $J_n(u, v)$ is

$$\begin{aligned} J_n(z^{1/2}\alpha, -\frac{1}{2}z) &\approx (2\pi QR)^{-1/2} (2z^{1/2})^n [(n+z+Q)^{1/2} + (n-3z+Q)^{1/2}]^{-n} \\ &\quad \times [(Q^{1/2} + U^{1/2})^{1/2} \cos\chi - (Q^{1/2} - U^{1/2})^{1/2} \sin\chi] \exp[RU^{1/2}/2 + 3\alpha(Q-U)^{1/2}/(32)^{1/2}], \quad (\text{D11}) \end{aligned}$$

where

$$\begin{aligned} \chi &= 3\alpha U^{1/2}/(32)^{1/2} - R(Q-U)^{1/2}/2 \\ &\quad - n \arccos[(n+z-Q)^{1/2}/2z^{1/2}], \\ Q &= [(n+z)^2 - z\alpha^2]^{1/2}, \quad (\text{D12}) \\ R &= (n-z - \frac{1}{8}\alpha^2)^{1/2}, \\ U &= \frac{1}{2}(n+z+Q) - \frac{1}{8}\alpha^2. \end{aligned}$$

$$\phi_0 = \phi_r + i\phi_i, \quad \phi_r, \phi_i \text{ real.}$$

Equation (D5) is equivalent to the two equations

$$\begin{aligned} \cos\phi_r \cosh\phi_i &= \alpha/4z^{1/2}, \\ \sin\phi_r \sinh\phi_i &= \mp [8(n-z) - \alpha^2]^{1/2}/4z^{1/2}. \quad (\text{D7}) \end{aligned}$$

These equations can be solved to give

$$\begin{aligned} \cos\phi_r &= (2z^{1/2})^{-1} \{ (n+z) - [(n+z)^2 - z\alpha^2]^{1/2} \}^{1/2}, \\ \sin\phi_r &= \pm (2z^{1/2})^{-1} \{ (3z-n) + [(n+z)^2 - z\alpha^2]^{1/2} \}^{1/2}, \quad (\text{D8}) \end{aligned}$$

$$\begin{aligned} \cosh\phi_i &= (2z^{1/2})^{-1} \{ (n+z) + [(n+z)^2 - z\alpha^2]^{1/2} \}^{1/2}, \\ \sinh\phi_i &= \pm (2z^{1/2})^{-1} \{ -(3z-n) + [(n+z)^2 - z\alpha^2]^{1/2} \}^{1/2}. \end{aligned}$$

Of the four saddle points that lie between $\phi_r = -\pi$ and $\phi_r = +\pi$, two lie above the real axis and the other two below. It is the latter two saddle points through which the original path of integration can be deformed, so that the integral can be evaluated by steepest-descent approximation.

The result of a steepest-descent approximation to the integral in Eq. (D2) can be written in general as

$$J_n(z^{1/2}\alpha, -\frac{1}{2}z) \approx \sum \frac{\exp[zg(\phi_0)]}{[-2\pi z g''(\phi_0)]^{1/2}}, \quad (\text{D9})$$

where the sum is carried out over the saddle points through which the steepest-descent path passes, and $g(\phi_0)$, $g''(\phi_0)$ are found from Eq. (D3) with the values (D8) substituted. The values of $\sin\phi_0$ which appear in $g(\phi_0)$, $g''(\phi_0)$ are

An alternate way to express Eq. (D11) arises from the relation

$$\begin{aligned} (2z^{1/2})^n [(n+z+Q)^{1/2} + (n-3z+Q)^{1/2}]^{-n} \\ = \exp[-n \operatorname{arcsinh}[(n-3z+Q)^{1/2}/2z^{1/2}]]. \quad (\text{D13}) \end{aligned}$$

Equation (D11) is the most general asymptotic form of $J_n(u, v)$ which follows from the conditions stated in Eq. (D1).

*Present address.

†Permanent address.

- ¹L. V. Keldysh, Zh. Eksp. Teor. Fiz. 47, 1945 (1964) [Sov. Phys.—JETP 20, 1307 (1965)].
- ²N. G. Basov, A. Z. Grasyuk, I. G. Zubarev, V. A. Katalin, and O. N. Krokhin, Zh. Eksp. Teor. Fiz. 50, 551 (1966) [Sov. Phys.—JETP 23, 366 (1966)].
- ³J. H. Yee, Phys. Rev. B 3, 355 (1971).
- ⁴F. Adduci, I. M. Catalano, A. Cingolani, and A. Minafra, Phys. Rev. B 15, 926 (1977).
- ⁵H. D. Jones and H. R. Reiss, Phys. Rev. B 16, 2466 (1977).
- ⁶H. R. Reiss, Phys. Rev. A 19, 1140 (1979).
- ⁷S. Geltman, J. Phys. B 10, 831 (1977).
- ⁸B. H. Armstrong, Phys. Rev. 131, 1132 (1963).
- ⁹L. A. Lompre, G. Mainfray, C. Manus, S. Repoux, and J. Thebault, Phys. Rev. Lett. 36, 949 (1976).
- ¹⁰H. R. Reiss, Phys. Rev. Lett. 29, 1129 (1972).
- ¹¹H. R. Reiss, J. Math. Phys. 3, 387 (1962).
- ¹²See, for example, L. I. Schiff, *Quantum Mechanics* (McGraw-Hill, New York, 1968), p. 446.
- ¹³This is true even if Ψ_A is used in its full form, without long-wavelength approximation. If long-wavelength approximation is not used, Ψ_A is not an eigenfunction of that component of momentum in the field propagation direction. However, V_A contains only transverse-momentum operators and so Eq. (8) remains true in general.
- ¹⁴This is the nonrelativistic limit of the intensity parameter denoted z_p in Ref. 6. It is exactly analogous to the parameter z introduced in Ref. 5.
- ¹⁵R. A. Fox, R. M. Kogan, and E. J. Robinson, Phys. Rev. Lett. 26, 1416 (1971).
- ¹⁶R. M. Kogan, R. A. Fox, G. T. Burnham, and E. J. Robinson, Bull. Am. Phys. Soc. 16, 1411 (1971).
- ¹⁷J. P. Hernandez and A. Gold, Phys. Rev. 156, 26 (1967).
- ¹⁸P. Lambropoulos, Phys. Rev. Lett. 28, 585 (1972).
- ¹⁹A. M. Perelomov, V. S. Popov, and M. V. Terent'ev, Zh. Eksp. Teor. Fiz. 50, 1393 (1966) [Sov. Phys.—JETP 23, 924 (1966)].
- ²⁰Y. Gontier and M. Trahin, Phys. Rev. A 7, 2069 (1973).
- ²¹J. R. Oppenheimer, Phys. Rev. 31, 66 (1928).
- ²²L. D. Landau and E. M. Lifshitz, *Quantum Mechanics* (Pergamon, Oxford, 1958), p. 258.
- ²³S. Geltman, J. Phys. B 11, 3323 (1978).
- ²⁴M. Göppert-Mayer, Ann. Phys. (Leipzig) 9, 273 (1931).
- ²⁵R. N. Hill, Phys. Rev. Lett. 38, 643 (1977).
- ²⁶See, for example, D. Park, *Introduction to the Quantum Theory* (McGraw-Hill, New York, 1974), pp. 299 and 306.
- ²⁷See, for example, E. Merzbacher, *Quantum Mechanics* (Wiley, New York, 1970), p. 471; or D. Park, *Introduction to the Quantum Theory* (McGraw-Hill, New York, 1974), p. 400. Note that Park orients the polar axis of angular coordinates along the direction of propagation of the field, rather than along the direction of polarization, as done in Eq. (109).
- ²⁸J. E. Rogerson, Ph.D. thesis, The American University, 1974 (unpublished).
- ²⁹H. R. Reiss, Phys. Rev. A 1, 803 (1970); Phys. Rev. Lett. 25, 1149 (1970). In these papers, the parameter used was $(\frac{2}{3}eaaa_0)^2$ for bound-bound transitions between 1S and 2S states. For bound-free or arbitrary bound-bound transitions, the generic parameter is $(eaa_0)^2$.
- ³⁰H. R. Reiss, Phys. Rev. Lett. 26, 1072 (1971).
- ³¹H. R. Reiss, Ph.D. thesis, University of Maryland, 1958 (unpublished).
- ³²H. R. Reiss, J. Math. Phys. 3, 59 (1962).
- ³³A. I. Nikishov and V. I. Ritus, Zh. Eksp. Teor. Fiz. 46, 776 (1964) [Sov. Phys.—JETP 19, 529 (1964)].
- ³⁴L. S. Brown and T. W. B. Kibble, Phys. Rev. 133, A705 (1964).